Abundance estimates of Antarctic minke whales from the historical IDCR/SOWER survey data using the OK method.

Hiroshi Okamura[1] and Toshihide Kitakado[2]

[1] National Research Institute of Far Seas Fisheries, Fisheries Research Agency, Kanagawa 236-8648, Japan

[2] Tokyo University of Marine Science and Technology, Minato, Tokyo 108-8477, Japan

The corresponding author's email address: okamura@fra.affrc.go.jp

ABSTRACT

This document presents the specifications of the latest OK method and the abundance estimates of Antarctic minke whales from the historical IDCR/SOWER survey data. The method is based on a design-based approach with the revised hazard probability model, which was applied to the data obtained by the surveys from 1985/86 to 2003/04. We carried out some sensitivity analyses: (1) the form of probability distributions for school size bias related to confirmation status, (2) the form of Q functions, and (3) different weather covariates (Sightability and Beaufort Class). The AIC best model had a truncated negative binomial model for IO mode and a truncated Poisson distribution for CL mode as a probability model of school size bias, a logistic form as a Q function, and Sightability for CPII and Beaufort Class for CPIII as a weather covariate. The abundance for each management area was estimated using the "survey-once" method. The total abundances in the survey areas were 1,485,724 (CV: 0.172) for CPII and 711,877 (CV: 0.165) for CPIII with the actual northern boundary of the surveyed strata.

1. INTRODUCTION

The International Decade of Cetacean Research - Southern Ocean Whale and Ecosystem Research (IDCR/SOWER) surveys have been conducted annually in the Antarctic since the 1970s. The sightings data of Southern Hemisphere minke whales (*Balaenoptera bonaerensis*) have been collected as one of main purposes of the IDCR/SOWER surveys. The sightings data consist of three circumpolar sets of cruises: 1978/79-1983/84 (1st circumpolar: CPI), 1985/86-1990/91 (2nd circumpolar: CPII), and 1991/92-2003/04 (3rd circumpolar: CPIII). The abundance estimates for Southern Hemisphere minke whales (*Balaenoptera bonaerensis*) were estimated by conventional line transect methods (Branch and Butterworth, 2001; Matsuoka et al., 2003; Branch, 2006). The abundance estimates for the 3rd circumpolar surveys obtained from the IDCR/SOWER data showed a dramatic decrease compared with the 2nd circumpolar surveys. Some members in the Scientific Committee of International Whaling Commission (IWC/SC) doubted whether it was the true decrease. Consequently, IWC/SC has listed a number of possible causes that might result in the change in estimates (IWC, 2002).

One of the important assumptions in conventional line transect sampling is that all animals on the line are detected without failure, i.e., the probability of seeing an animal if it occurs on the survey trackline, commonly called $g(0)$, is equal to 1. However, the diving behaviour of cetaceans can lead to this assumption being violated, even if the animal occurs on the trackline. Since minke whales are relatively small baleen whales, it is often difficult for observers on the sighting vessel to detect them so that $g(0)$ tends to be less than 1 (Schweder et al., 1997; Skaug et al., 2004; Okamura et

al., 2003, 2005). IWC (2002) suggested that the difference of the abundance estimates of Branch and Butterworth (2001) would possibly be attributed to changes in $g(0)$ to some extent. Fortunately, the IDCR/SOWER surveys have conducted double-platform line transect sampling with independent observers, which gives the information needed to estimate $g(0)$. In this paper, we provide the revised abundance estimates of CPII and CPIII with $g(0)$ estimation by independent observer data.

There is a remarkable difference in mean school sizes between CPII and CPIII data (Branch and Butterworth, 2001; IWC, 2002). Mean school sizes could be overestimated if one uses a conventional line transect method with $g(0) = 1$ when $g(0)$ is in fact less than 1. Since $g(0)$ and mean school size are closely related to each other (Cooke, 1985; Butterworth, 2002), the trend and abundance estimates of Southern Hemisphere minke whales could be miscalculated unless there is an appropriate allowance for $g(0)$ and bias in mean school size. The survey effort of IDCR/SOWER surveys is divided into the Closing and IO modes. In the Closing mode, when a school of whales is detected, the vessel turns off the trackline and closes with the sighting to confirm the school size and species. The Closing mode data therefore provide more accurate information on school size, while the IO mode data are representative of double-platform line transect sightings collected by independent observers. Okamura et al. (2005) gave a basic model to estimate $g(0)$ and a school size distribution for IDCR/SOWER data dealing with the Closing and IO mode data together in their analysis method. Okamura and Kitakado (2008a) modified their model and showed that it could provide relatively small bias of abundance estimates for the simulated data produced by IWC (Palka and Smith, 2004, 2005). We use the basic structure of a hazard probability model used in Okamura and Kitakado (2009) for the real IDCR/SOWER datasets to estimate the abundance estimates. We added three main changes to the model and the used data: (1) the use of whole data by circumpolar sets, (2) the introduction of a new form of probability distributions for school size bias related to confirmation status, and (3) taking account of Sightability as well as Beaufort Sea State.

The next section describes the data and the methodology used in this paper. The mathematical details of the model are given in Appendices. Section 3 presents the results and discussion.

2. MATERIALS AND METHODS

2.1. The data

We used the IDCR/SOWER standard dataset extracted from DESS by M. L. Burt (July 27, 2005). We basically followed the procedure in Branch and Butterworth (2001, 2006) as far as possible to process data for analysis. However, when we had some differences in the procedure due to the difference of the analysis methods, we handled the data in a fashion unique to ourselves. For example, we used duplicate sightings to estimate $g(0)$ and confirmed school sizes in the IO and Closing modes to estimate school size distribution unlike Branch and Butterworth (2001). The details of our procedure were as follows.

Circumpolar set

We used 1985/86 - 2003/04 data, which corresponded to CPII and CPIII.

Stratum

We used the new stratum boundary produced by Mark Bravington.

Vessel Speed

The vessel speeds recorded in the effort records were used. They were not constant during the surveys. When the value was 888 (variable speed) or 999 (missing), we used the preset speed, 12 knot (before 1986/87) and 11.5 knot (after 1987/88). When calculating esw, the preset speed was used.

Survey effort

The survey effort was calculated by the vessel speed times the traveled time in the effort records. We used all the data with different activity codes without excluding the codes "BH" and "BL" according to Branch (2006).

Species

We used data with the species code 04, 91, 92, 39. "Like minke" was included.

Sea state

Sightability and Beaufort were adopted as possible covariates. We used two levels for both covariates. The details are given in the sensitivity analysis below.

Platform

The original category was the following: 1 - topman in standard barrel, 2 - topman in IO position, 3 - upper bridge, primary observer, 4 - upper bridge, not primary observer, 5 - 1 and 4 simultaneously, 6 - 2 and 4 simultaneously.

We used a new category in that 1 & 5 $\rightarrow$ A, 2 & 6 $\rightarrow$ B, and 3 & 4 $\rightarrow$ C as in Appendix B.

Sighting distances and angles

Bias-corrected distances and angles were used. Angles were truncated at 90 degrees and transformed to radian. We used the perpendicular and forward distances transformed from the radial distances and angles in the analysis. The perpendicular distances transformed were truncated at 1.5 nautical miles, while the forward distances were not truncated.

School size

Best school size estimates were used.

Duplicate

Duplicate sightings in the IO-tracking searching under closing mode in 1987/88 were removed.

We adopted "definite" duplicates as the true duplicates under IO mode. When any covariate other than sighting distances and angles was different in a duplicate sighting, we conformed to the following rules:

- School size: If confirmed school size was only one, we used the value. If there were multiple confirmed school sizes or no confirmed school size, we then used the value of the platform with the highest sighting position based on the notion that a topman was the most reliable.
- Confirmation status of school size: If we had at least one confirmed school size, it was defined as confirmed.

- Sea state: When the sea states were different, we adopted the sea state with the earlier record time.

The case with different covariates by different platforms in a duplicate sighting was few and therefore the above minor adjustment will have little effect on abundance estimation.

Truncation

Perpendicular distances were truncated at 1.5 nautical miles according to conventional method (Branch and Butterworth, 2001). When the sightings were duplicates, we used the averaged distances for the simultaneous duplicates and the distances of later sightings for the delayed duplicates.

2.2. The hazard probability model and the likelihood function

The detection probability density function of the animal positioned at the perpendicular distance x and the forward distance y assuming a Poisson surfacing pattern with the mean surfacing rate λ is

$$p(x,y) = \frac{\lambda}{v} Q(x,y) \exp\left\{-\frac{\lambda}{v}\int_y^\infty Q(x,y')dy'\right\}, \tag{1}$$

where v is the vessel speed, and $Q(x,y)$ is a hazard probability function based on a logistic function (Appendix A). The parameters in Eq. (1) are linked to various factors. Vessel, true school size, weather conditions (Beaufort or Sightability), and platforms were employed as the covariates for a detection process, while stratum and distance from the ice edge were linked with mean school size (Appendices A and B). We used Gaussian integration for all the integrals hereafter. In addition, we used Gaussian summation for $\sum_{s=1}^{\infty}$ (Monien 2006).

We construct a likelihood function conditioned on detection patterns and confirmation status of school size (Appendix B). For the confirmed school size, the likelihood function is

$$P_C(x_i, y_i, u_i, s_i) = \frac{c_k p_k(x_i, y_i, u_i|s_i)\pi(s_i)}{\mathrm{esw}_k}, \tag{2}$$

and for the unconfirmed school size, the likelihood function is

$$P_U(x_i, y_i, u_i, z_i) = \frac{\sum_{s=1}^{\infty}(1-c_k)\rho(z_i|s)p_k(x_i, y_i, u_i|s)\pi(s)}{\mathrm{esw}_k}, \tag{3}$$

where k is an index that denotes Passing/Closing mode, c_k is the probability of school size confirmation dependent on some covariates such as true school size, $\rho(z_i|s)$ is the probability that the school size is recorded as z_i given the true school size is s and the observed school size z_i is unconfirmed. u_i is a type of detection pattern, p_k is a detection probability density function given the mode k and the detection pattern u_i, and $\pi(s)$ is a probability mass function of true school size, and esw_k is

$$\mathrm{esw}_k = \int_0^{x_{max}} \int_0^\infty \sum_{s=1}^{\infty} \sum_{u}^{\text{all patterns}} p_k(x, y, u|s)\pi(s)dxdy. \tag{4}$$

For the simplification of calculation, when $z_i \geq z_{max}$, the above probability for the unconfirmed school size is modified to

$$P_U(x_i, y_i, u_i, z_i \geq z_{max}) = \frac{\sum_{s=1}^{\infty}(1-c_k)\{1-\sum_{z=1}^{z_{max}-1}\rho(z|s)\}p_k(x_i, y_i, u_i|s)\pi(s)}{\mathrm{esw}_k}. \quad (5)$$

The mean value of true school size distribution, $\pi(s)$, is linked to the interaction of circumpolar set and survey area, and the logarithm of distance from the ice edge (Appendix C). The confirmation probability is dependent on survey mode, weather condition, perpendicular distance (for IO mode) and radial distance (for Closing mode) (Appendix C).

The total likelihood function is then given by

$$L = \prod_{i=1}^{n_C} P_C(x_i, y_i, u_i, s_i) \times \prod_{i=1}^{n_U} P_U(x_i, y_i, u_i, z_i), \quad (6)$$

where n_C and n_U are the numbers of the sightings with confirmed and unconfirmed school size, respectively. We estimate parameters by maximizing the logarithm of the total likelihood function. The maximization of the likelihood function is conducted separately for each Management Area and Circumpolar Set.

2.3. Abundance estimation

We use only the IO mode data in abundance estimation to circumvent possible biases that the Closing mode data involve (Kishino and Kasamatsu, 1987; Branch and Butterworth, 2001), while we use both of the Closing and IO mode data for parameter estimation as above mentioned. The population size is then estimated with a Horvitz-Thompson-like estimator,

$$\hat{P} = \frac{A}{2L}\sum_{i=1}^{n_P}\frac{\phi_1(\eta_i)+1}{\sum_{s=1}^{\infty}\hat{\mathrm{esw}}_{A\cup B\cup C}(s|\eta_i)\hat{\pi}(s|\eta_i)}, \quad (7)$$

where n_P is the number of the sightings in the IO mode, L is total survey distance, A is the size of survey area, η_i is a vector of covariates except for school sizes, and the numerator corresponds to the mean school size derived from a parametric distribution of school size (Appendix C).

An estimator for the unconditional asymptotic variance of $\hat{P}$ is then

$$\hat{\mathrm{var}}(\hat{P}) = \left[\left\{\frac{d\hat{P}(\theta)}{d\theta}\right\}^T I(\theta)^{-1}\frac{d\hat{P}(\theta)}{d\theta}\right]_{\theta=\hat{\theta}} + \frac{A^2}{J-1}\sum_{j=1}^{J}\frac{l_j}{L}(\hat{D}_j - D)^2, \quad (8)$$

where θ is a vector of estimated parameters, $I(\theta)$ is the Fisher information matrix obtained from the second derivative of the log-likelihood function that is often substituted by the Hessian matrix, and l_j $(j = 1, \ldots, J; \sum l_j = L)$ is a replicated line. $\hat{D}_j$ is the density on replicate line j. If there is no sighting on replicate line j, $\hat{D}_j$ is defined as being equal to zero.

When the abundance estimates are obtained by strata, taking account of common estimated parameters across strata, the abundance estimate and its variance for the whole area are given by

$$\hat{P}_{\text{all strata}} = \sum_h A_h \hat{D}_h, \tag{9}$$

$$\hat{\text{var}}(\hat{P}_{\text{all strata}}) = \left[\left\{ \frac{d\hat{P}_{\text{all strata}}(\theta)}{d\theta} \right\}^T I(\theta)^{-1} \frac{d\hat{P}_{\text{all strata}}(\theta)}{d\theta} \right]_{\theta=\hat{\theta}} + \sum_h \frac{A_h^2}{J_h - 1} \sum_{j=1}^{J_h} \frac{l_{j,h}}{L_h} (\hat{D}_{j,h} - D_h)^2, \tag{10}$$

where the subscript h is the index of stratum.

The covariance between abundance estimates with different years taking account of common parameters is calculated by

$$\hat{\text{cov}}(\hat{P}_1, \hat{P}_2) = \left[\left\{ \frac{d\hat{P}_1(\theta)}{d\theta} \right\}^T I(\theta)^{-1} \frac{d\hat{P}_2(\theta)}{d\theta} \right]_{\theta=\hat{\theta}}, \tag{11}$$

where the subscripts denote different years and areas. The correlation matrix is obtained from the estimated variances and covariances. The additional variance is added to the estimated variances (Kitakado and Okamura, 2005, 2008, 2009). The final abundances for management areas were calculated using the estimates based on the additional variance blocks.

2.4. Sensitivity analysis

We conducted some sensitivity analyses. The first one was on the probability mass function of unconfirmed school size given true school size. We tested six types of models with difference of Poisson or negative binomial, of whether the bias parameter is dependent on true school size or not, and whether the truncation distribution is the probability of school size – 1 or the usual one. The second one was the effect of Q function form. The logistic form and the separate product form were used. The third one was to investigate which weather condition covariate should be used. Beaufort Sea State and Sightability were taken into account.

In addition, we conducted the analysis by eliminating upper bridge platform to examine the effect of fit of radial distances.

3. RESULTS AND DISCUSSION

We used the model given in Appendices A–C for abundance estimation. The selection process of AIC suggested that the model that has a usual truncated negative binomial distribution for IO mode and a usual truncated Poisson distribution for Closing mode as probability distributions for school size bias related to confirmation status with the β parameter depending on true school size, a logistic Q function, and Sightability for CPII and Beaufort for CPIII as a weather covariate, was the best one (Tables 1 – 3).

Tables 4 – 7 provide necessary basic information on g(0), esws, and abundances. g(0)s were generally between 0.4 and 0.5. The additional CV was estimated to be 0.413 (Table 8). The survey-once abundance estimates taking account of additional variance (Kitakado and Okamura 2009) were

1,485,724 (CV: 0.172) for CPII and 711,877 (CV: 0.165) for CPIII with the actual northern boundary of the surveyed strata, when we use the definite duplicates only (Table 8). The results were not so different from the last year's ones, but the CPII abundance increased to some degree. This change would be due to increase of mean school size as a result of change to the probability mass function of unconfirmed school size given true school size.

The graphical diagnostic plots were given for the best model (Figs. 1 – 5). The overall goodness of fits was not so different from the last year (Okamura and Kitakado 2009). Figs. 6 – 7 show the effect on radial distances by platform. Platform C (Upper Bridge) has most contributed to small radial distances. When the model was fitted to data excluding Platform C, the fitting of radial distances is slightly improved, but it was not a big change (Fig. 8). The abundance estimates excluding Platform C were slightly smaller than those including Platform C (Table 9).

ACKNOWLEDGMENTS

We greatly thank Mark Bravington for the CNB program and the revised stratum boundary.

REFERENCES

Branch, T. A. (2005) Combining estimates from the third circumpolar set of survey. J. Cetacean Res. Manage. **7** (Suppl.): 231-233.

Branch, T. A. (2006) Abundance estimates for Antarctic minke whales from three completed circumpolar sets of surveys, 1978/79 to 2003/04. Paper SC/58/IA18 presented to the IWC/SC (unpublished): 28pp.

Branch, T. A. and Butterworth, D. S. (2001) Southern Hemisphere minke whales: standardised abundance estimates from the 1978/79 to 1997/98 IDCR-SOWER surveys. J. Cetacean Res. Manage. **3**: 143-174.

Branch, T. A. and Butterworth, D. S. (2006) Suggested options for the analysis of IDCR/SOWER minke whale data. Paper SC/58/IA19 presented to the IWC/SC (unpublished): 10pp.

Butterworth, D. S. (2002) On bias in IDCR/SOWER estimates of abundance of minke whales which assume $g(0) = 1$. J. Cetacean Res. Manage. **4** (Suppl.): 229.

Cooke, J. G. (1985) Notes on the estimation of whale density from line transects. Rep. int. Whal. Commn **35**: 319-323.

Cooke, J. G. (1997) An implementation of a surfacing-based approach to abundance estimation of minke whales from shipborne surveys. Rep. int. Whal. Commn **47**: 513-528.

Cooke, J. G. (2001) A modification of the radial distance method for dual-platform line transect analysis to improve robustness. Paper SC/53/IA31 presented to the IWC/SC (unpublished): 7pp.

International Whaling Commission (2002) Report of the sub-committee on the comprehensive assessmnet of whale stocks - in-depth assessments. J. Cetacean Res. Manage. **4** (Suppl.): 192-229.

International Whaling Commission (2008) Report of the SOWER Abundance Workshop.

Kishino, H. and Kasamatsu, F. (1987) Comparison of the closing and passing mode procedures used in sighting surveys. Rep. int. Whal. Commn **37**: 253-258.

Kitakado, T. and Okamura, H. (2005) Estimation methods of the additional variance for Antarctic minke whales. Paper SC/57/IA5 presented to the IWC/SC (unpublished): 7pp.

Kitakado, T. and Okamura, H. (2008) Some issues on the additional variance. Paper SC/F08/A11 presented to the SOWER Abundance Workshop (unpublished): 5pp.

Kitakado, T. and Okamura, H. (2009) Estimation of additional variance for Antarctic minke whales based on the abundance estimates from the revised OK method. Paper SC/61/IA8 presented to the IWC/SC meeting (unpublished): 11pp.

Matsuoka, K., Ensor, P., Hakamada, T., Shimada, H., Nishiwaki, S., Kasamatsu, F. and Kato, H. (2003). Overview of minke whale sightings surveys conducted on IWC/IDCR and SOWER Antarctic cruises from 1978/79 to 2000/01. J. Cetacean Res. Manage. 5:173-201.

Monien, H. (2006) Gaussian summation: an exponentially convergent summation scheme. arXiv:math/0611057v1. Available at http://arxiv.org/PS cache/math/pdf/0611/0611057v1.pdf.

Okamura, H., Kitakado, T., Hiramatsu, K., and Mori, M. (2003) Abundance estimation of diving animals by the double-platform line transect method. Biometrics **59**: 512-520.

Okamura, H., Kitakado, T., and Mori, M. (2005) An improved method for line transect sampling in Antarctic minke whale surveys. J. Cetacean Res. Manage. **7**: 97-106.

Okamura, H. and Kitakado, T. (2007a) Simulation results of Southern Hemisphere minke whale abundance surveys using a hazard probability model. Paper SC/59/IA15 presented to the IWC/SC (unpublished): 12pp.

Okamura, H. and Kitakado, T. (2007b) Abundance estimates of Southern Hemisphere minke whales from the IDCR/SOWER surveys using a hazard probability model. Paper SC/59/IA14 presented to the IWC/SC (unpublished): 29pp.

Okamura, H. and Kitakado, T. (2008a) Summary of simulation trials of Antarctic minke whale abundance surveys using the OK method. Paper SC/60/IA10 presented to the IWC/SC (unpublished).

Okamura, H. and Kitakado, T. (2008b) Graphical diagnosis for the IDCR/SOWER abundance estimates using the OK method. Paper SC/60/IA9 presented to the IWC/SC (unpublished).

Okamura, H. and Kitakado, T. (2009) Abundance estimates and diagnostics of Antarctic minke whales from the historical IDCR/SOWER survey data using the OK method. Paper SC/61/IA6 presented to the IWC/SC (unpublished).

Palka, D. L. and Smith, D. W. (2004) Simulating the IDCR/SOWER surveys - 2004. Paper SC/56/IA6

presented to the IWC/SC (unpublished): 16pp.

Palka, D. L. and Smith, D. W. (2005) Description of 2005 simulations of the IWC/SOWER Southern Hemisphere minke whale abundance surveys. Paper SC/57/IA2 presented to the IWC/SC (unpublished): 8pp.

Schweder, T., Skaug, H. J., Dimakos, X. K., Langaas, M., and Oien, N. (1997). Abundance of northeastern Atlantic minke whales, estimates for 1989 and 1995. Rep. int. Whal. Commn **47**: 453-483.

Skaug, H. J., Oien, N., Schweder, T., and Bothun, G.. (2004) Abundance of minke whales (Balaenoptera acutorostrata) in the Northeast Atlantic: variability in time and space. Can. J. Fish. Aquat. Sci. **61**: 870-886.

Appendix A detection probability function of sighting cues

The hazard probability model is given by a logistic form,

$$Q(x,y) = \frac{1}{1+\exp[\tau_r R^{\gamma_r} + \tau_a A^{\gamma_a} + \omega]} \tag{A.1}$$

where $R = \sqrt{x^2+y^2}$, $A = \text{atan}(x/y)$, x is the perpendicular distance, y is the forward distance, τ_r, τ_a, γ_r, and γ_a are scalar parameters with positive values. The parameters, τ_r, τ_a, and ω, are related to several covariates through a link function as follows:

$\log(\tau_r) \sim$ Platform + log(School.size) + Weather,

$\log(\tau_a) \sim$ Platform + log(School.size) + Weather,

$\omega \sim$ Platform + log(School.size) + Weather + Vessel.

In addition, the surfacing rate λ in Eq. (1) is modeled to be a function of school size,

$\log(\lambda) \sim$ log(School.size),

where the coefficient of log(School.size) is constrained to be positive.

Appendix B Specification of detection function for each sighting pattern

There are three platforms with two independent observers and one semi-independent observer in the IO mode while there are two platforms with no independent observer in the Closing mode. The detection pattern in the IO mode is therefore complicated by taking account of duplicate sightings.

B-1. IO mode

IO mode has three sighting platforms, the top barrel and the IO booth with independent observers, and the upper bridge with semi-independent observers or researchers. We can have information needed to estimate $g(0)$ from the sighting patterns of independent observers (Schweder et al., 1997; Cooke, 1997; Cooke, 2001; Okamura et al., 2003, 2005). The probability density function for each sighting pattern is given below. The contribution to the likelihood function of detection with each sighting pattern is calculated by each probability density times the probability mass density of school size (Appendix C) divided by $\text{esw}_{A\cup B\cup C}$ when school sizes are confirmed. When school sizes are unconfirmed, the numerator is summed up over all school sizes. $\text{esw}_{A\cup B\cup C}$ is given by

$$\begin{aligned}\text{esw}_{A\cup B\cup C} = \sum_{s=1}^{\infty}\Bigg[\int_0^{x_{max}}\int_0^{\infty}\frac{\lambda}{v}Q_{A\cup B\cup C}(x,y|s) \\ \times\exp\left\{-\frac{\lambda}{v}\int_y^{\infty}Q_{A\cup B\cup C}(x,y'|s)dy'\right\}dxdy\Bigg]\pi(s),\end{aligned} \tag{B.1}$$

which is equal to Eq. (4) when $k =$ IO mode.

We have two distances by independent observers in the delayed duplicates. We use the averaged distances for the simultaneous duplicates and the distances of the latter sightings for the delayed duplicates, since the latter sightings tend to have the distances closer to the vessel which are generally likely to be more accurate. The distances of the first sightings are calculated by adding the vessel speeds times the differences of the recorded times between the two sightings to the distances of the latter sightings.

In the IDCR/SOWER surveys before 1988/89, the sighting time was recorded in a "minute" unit, and "second" was omitted. We therefore add to the model to apply to the data before 1988/89

the additional sturcture taking account of uncertainty by rounding the sighting time to the nearest minute.

1. A

$$p(x,y,A) = \frac{\lambda}{v}\left\{Q_{A\cup B}(x,y) - Q_B(x,y)\right\}\exp\left\{-\frac{\lambda}{v}\int_0^y Q_B(x,y')dy'\right\}$$
$$\times\exp\left[-\frac{\lambda}{v}\left\{\int_y^\infty Q_{A\cup B}(x,y')dy' + \int_{y+vT}^\infty Q_{A\cup B\cup C\setminus A\cup B}(x,y')dy'\right\}\right], \tag{B.2}$$

where $T = 90/3600$h (before 1988/89) and $T = 60/3600$h (after 1989/90).

2. B

Same as A except for exchanging the symbols A and B.

3. C

$$p(x,y,C) = \frac{\lambda}{v}\left\{Q_{A\cup B\cup C}(x,y) - Q_{A\cup B}(x,y)\right\}$$
$$\times\exp\left[-\frac{\lambda}{v}\left\{\int_0^y Q_{A\cup B}(x,y')dy' + \int_y^\infty Q_{A\cup B\cup C}(x,y')dy'\right\}\right]. \tag{B.3}$$

4. $A\times B$

$$p(x,y,AB) = \frac{\lambda}{v}\left(Q_A(x,y)Q_B(x,y)\exp\left\{-\frac{\lambda}{v}\int_y^\infty Q_{A\cup B}(x,y')dy'\right\}\right.$$
$$+Q_A(x,y)\exp\left\{-\frac{\lambda}{v}\int_y^\infty Q_A(x,y')dy'\right\}$$
$$\times\left[\exp\left\{-\frac{\lambda}{v}\int_{y+vT}^\infty Q_{A\cup B\setminus A}(x,y')dy'\right\} - \exp\left\{-\frac{\lambda}{v}\int_y^\infty Q_{A\cup B\setminus A}(x,y')dy'\right\}\right]$$
$$+Q_B(x,y)\exp\left\{-\frac{\lambda}{v}\int_y^\infty Q_B(x,y')dy'\right\}$$
$$\left.\times\left[\exp\left\{-\frac{\lambda}{v}\int_{y+vT}^\infty Q_{A\cup B\setminus B}(x,y')dy'\right\} - \exp\left\{-\frac{\lambda}{v}\int_y^\infty Q_{A\cup B\setminus B}(x,y')dy'\right\}\right]\right) \tag{B.4}$$

where $T = 90/3600$h (before 1988/89) and $T = 60/3600$h (after 1989/90).

5. $A\to B$

For the dataset before 1988/89,

$$p(x,y,A\to B) = \frac{\lambda}{v}$$
$$\times\left[\exp\left\{-\frac{\lambda}{v}\int_{y+v(\tau_{AB}+T)}^\infty Q_{A\cup B\setminus B}(x,y')dy'\right\} - \exp\left\{-\frac{\lambda}{v}\int_{y+v(\tau_{AB}-T)}^\infty Q_{A\cup B\setminus B}(x,y')dy'\right\}\right]$$
$$\times Q_B(x,y)\exp\left\{-\frac{\lambda}{v}\int_y^\infty Q_B(x,y')dy'\right\} \tag{B.5}$$

where $T = 30/3600$h and $\tau_{AB}\geq 120/3600$h.

For the dataset after 1989/90,

$$p(x,y,A\to B)=\left(\frac{\lambda}{v}\right)^2 Q_B(x,y)\{Q_{A\cup B}(x,y+v\tau_{AB})-Q_B(x,y+v\tau_{AB})\}$$
$$\times\exp\left[-\frac{\lambda}{v}\left\{\int_{y+v\tau_{AB}}^{\infty}Q_{A\cup B\setminus B}(x,y')dy'+\int_y^{\infty}Q_B(x,y')dy'\right\}\right] \tag{B.6}$$

where $\tau_{AB} > 60/3600$h.

6. $B \to A$

Same as $A \to B$ for exchanging the symbols A and B.

7. $C \to A$

For the dataset before 1988/89,

$$p(x,y,C\to A)=\frac{\lambda}{v}\left[\exp\left\{-\frac{\lambda}{v}\int_{y+v(\tau_{CA}+T)}^{\infty}Q_{A\cup B\cup C\setminus A\cup B}(x,y')dy'\right\}-\right.$$
$$\left.\exp\left\{-\frac{\lambda}{v}\int_{y+v(\tau_{CA}-T)}^{\infty}Q_{A\cup B\cup C\setminus A\cup B}(x,y')dy'\right\}\right]$$
$$\times\{Q_{A\cup B}(x,y)-Q_B(x,y)\}$$
$$\exp\left[-\frac{\lambda}{v}\left\{\int_y^{\infty}Q_{A\cup B}(x,y')dy'+\int_0^{y}Q_B(x,y')dy'\right\}\right] \tag{B.7}$$

where $T = 30/3600$h and $\tau_{CA} \geq 120/3600$h.

For the dataset after 1989/90,

$$p(x,y,C\to A)=\left(\frac{\lambda}{v}\right)^2\{Q_{A\cup B}(x,y)-Q_B(x,y)\}$$
$$\times\{Q_{A\cup B\cup C}(x,y+v\tau_{CA})-Q_{A\cup B}(x,y+v\tau_{CA})\}$$
$$\times\exp\left\{-\frac{\lambda}{v}\int_{y+v\tau_{CA}}^{\infty}Q_{A\cup B\cup C\setminus A\cup B}(x,y')dy'\right\}$$
$$\times\exp\left[-\frac{\lambda}{v}\left\{\int_y^{\infty}Q_{A\cup B}(x,y')dy'+\int_0^{y}Q_B(x,y')dy'\right\}\right] \tag{B.8}$$

where $\tau_{CA} > 60/3600$h.

8. $C \to B$

Same as $C \to A$ for exchanging the symbols A and B.

B-2. Closing mode

We have two platforms, top barrel and upper bridge, for Closing mode. Once any observer on either platform detect the animal, the sighting is communicated to other observers by the researcher immediately. Hence, there are no duplicates in the Closing mode. The detection function is given by

$$p(x,y,A\cup C)=\frac{\lambda}{v}Q_{A\cup C}(x,y)\exp\left\{-\frac{\lambda}{v}\int_y^{\infty}Q_{A\cup C}(x,y')dy'\right\}. \tag{B.9}$$

The contribution to the likelihood function of detection with each sighting pattern is calculated by the above probability density times the probability mass density of school size (Appendix C) divided

by $\mathrm{esw}_{A\cup C}$ when school sizes are confirmed. When school sizes are unconfirmed, the numerator is summed up over all school sizes. $\mathrm{esw}_{A\cup C}$ is given by

$$\mathrm{esw}_{A\cup C} = \sum_{s=1}^{\infty} \left[\int_0^{x_{xmax}} \int_0^{\infty} \frac{\lambda}{v} Q_{A\cup C}(x, y|s) \right.$$
$$\left. \times \exp\left\{ -\frac{\lambda}{v} \int_y^{\infty} Q_{A\cup C}(x, y'|s) dy' \right\} dxdy \right] \pi(s), \tag{B.10}$$

which is equal to Eq. (4) when $k =$ Closing mode.

Appendix C Scool size distribution

The probability mass function of true school size is given by a truncated negative binomial distribution,

$$\pi(s) = \frac{\Gamma(\phi_0 + s - 1)}{\Gamma(\phi_0)\Gamma(s)} \left(1 - \frac{\phi_0}{\phi_0 + \phi_1}\right)^{s-1} \left(\frac{\phi_0}{\phi_0 + \phi_1}\right)^{\phi_0}, \tag{C.1}$$

where $\phi_0 > 0$, $\phi_1 > 0$, and the parameter ϕ_1 is linked to the following covariates,

$\log(\phi_1) \sim$ W/E Strata +W/E Strata $\times \log(d_{\mathrm{ice}} + 1.0)$, where $\mathrm{E}(s) = \phi_1 + 1$, and d_{ice} is the distance from the ice edge, which is used to represent the latitudinal gradient of school size. W/E Strata represents strata with similar longitudinal regions. The category of W/E Strata is as follows:

CPII
1: 1990WN, 1990WS
2: 1990EN, 1990ESBA
3: 1987WS1, 1987WS2, 1987WBAY
4: 1987WS3, 1987WN
5: 1987ES1, 1987ES2, 1987EBAY, 1987EM, 1987EN
6: 1988WN, 1988WS
7: 1988EN, 1988ES
8: 1989WN, 1989WS, 1989BN, 1989BS
9: 1989EN, 1989ES
10: 1986WN, 1986WM, 1986WS
11: 1986EN, 1986EM, 1986ES
12: 1991WN, 1991WS
13: 1991EN, 1991ES

CPIII
1: 1994WN, 1994WS
2: 1994EN, 1994ES
3: 200WN, 2000WS
4: 200EN, 2000ES
5: 2001EN, 2001ES
6: 1997WN, 1997WS

7: 1997EN, 1997ES
8: 1998WN, 1998WS, 2000ESA
9: 1998EN1, 1998EN2, 1998ES1, 1998ES2
10: 1993WN, 1993WS
11: 1993EN, 1993ES
12: 1995WN, 1995WS
13: 1995ENW, 1995ESW
14: 1995ENE, 1995ESE, 1995PRYD
15: 1999WN, 1999WS
16: 1999EN, 1999ES
17: 1992WN, 1992WS
18: 1992EN, 1992ES
19: 2002WN, 2002WS
20: 2002EN, 2002ES, 2002ESA
21: 2003W1N, 2003W1S
22: 2003W2N, 2003W2S
23: 2003EN, 2003ES
24: 2004N1, 2004N2, 2004N3, 2004MID, 2004ROSS
25: 1996WN, 1996WS
26: 1996EN, 1996ES
27 2001WN, 2001WS

The probability mass function of unconfirmed school size given true school size is given by a truncated Poisson or negative binomial distribution. We use two forms of truncated distributions. One is the probability distribution of school size – 1, for example a truncated Poisson distribution is

$$\rho(z|s) = \frac{\mu^{z-1}\exp(-\mu)}{\Gamma(z)}, \tag{C.2}$$

where $\mu = \beta(s-1) > 0$ and the parameter β is linked to the following covariates,

$\log(\beta) \sim$ School size + Survey.mode.

Note that $\mathrm{E}(z) = \mu + 1$.

The other is the probability distribution of school size, for example a truncated Poisson distribution is

$$\rho(z|s) = \frac{\mu^{z}\exp(-\mu)}{\Gamma(z+1)\{1-\exp(-\mu)\}}, \tag{C.3}$$

where $\mu = \beta s > 0$ and the parameter β is linked to the following covariates,

$\log(\beta) \sim$ School size + Survey.mode.

Note that $\mathrm{E}(z) = \mu/\{1-\exp(-\mu)\}$.

The probability of confirmation status c_k, which is given separately for each survey mode, is linked to the following covariates,

$\mathrm{logit}(c_k) \sim \log(s) + \sqrt{x^2+y^2}$ + Weather (for Closing mode),

$\mathrm{logit}(c_k) \sim \log(s) + x$ + Weather (for IO mode).

Table 1. Comparison among the confirmation probability models.

CPII

Truncation type	IO	CL	AIC	ΔAIC
1	P	P	25721.2	113.4
1	NB	NB	25624.4	16.6
1	NB with linear trend	NB with linear trend	25612.6	4.8
2	P	P	25696.2	88.4
2	NB	P	25668.2	60.4
2	**NB with linear trend**	**P with linear trend**	**25607.8**	**0**

CPIII

Truncation type	IO	CL	AIC	ΔAIC
1	P	P	27182.6	157.6
1	NB	NB	27048.8	23.8
1	NB with linear trend	NB with linear trend	27046.4	21.4
2	P	P	27192.4	167.4
2	NB	P	27105.6	80.6
2	**NB with linear trend**	**P with linear trend**	**27025.0**	**0**

Table 2. Comparison between two detection functions.

CPII

detection function	AIC	ΔAIC
logit	**25607.8**	**0.0**
separate	25654.2	46.4

CPIII

detection function	AIC	ΔAIC
logit	**27025.0**	**0.0**
separate	27069.2	44.2

Table 3. Comparison between Sightability and Beaufort.

CPII

weather	boundary	AIC	ΔAIC
BF	good (<3), bad (≥3)	25607.8	8.0
BF	good (<4), bad (≥4)	25630.2	30.4
SA	**good (≥4), bad (<4)**	**25599.8**	**0.0**
SA	good (≥3), bad (<3)	25603.0	3.2

CPIII

weather	boundary	AIC	ΔAIC
BF*	good (<3), bad (≥3)	27013.4	19.0
BF*	**good (<4), bad (≥4)**	**26994.4**	**0.0**
SA	good (≥4), bad (<4)	27002.2	7.8
SA	good (≥3), bad (<3)	27040.6	46.2

* Because the number of SA data is less than BF by one datum for CPIII, the model was fitted to the reduced data.

Table 4a. (D1, 2; A1) Abundance estimates of minke whales obtained from the IO mode data in Area 1 using the revised boundaries. Only the definite duplicates were used. See the text for the detailed explanation of parameters. The symbols used in this table denote the following:

Area: stratum area (n.miles2)
L: line length (primary search effort, n.miles)
nL: number of transects
ns: number of schools sighted (primary effort)
E(s): estimated mean school size
g(0): g(0) for the combined platforms
esw_s: effective strip-half width for schools by the combined platforms
esw_w: effective strip-half width for whales by the combined platforms
P: abundance estimate
D: density of whales
CV: coefficient of variation of abundance estimate

Area 1	Stratum	Area	L	nL	ns	E(s)	g(0)	esw_s	esw_w	P	D	CV
CP II												
1989/90	EN	154,323	750.2	7	60	1.559	0.443	0.209	0.308	46,375	0.301	0.221
	ESBA	63,236	821.1	14	74	2.668	0.540	0.321	0.561	23,486	0.371	0.475
	WN	170,142	577.9	6	35	6.546	0.644	0.492	1.085	67,873	0.399	0.559
	WS	45,571	830.9	15	214	3.649	0.549	0.348	0.676	60,314	1.324	0.212
	Total	433,272	2980.1	42	383					198,048	0.457	0.229
CP III												
1993/94	EN	295,236	749.6	10	17	1.785	0.523	0.356	0.561	16,900	0.057	0.789
	ES	73,028	544.8	9	84	1.772	0.460	0.291	0.479	34,564	0.473	0.371
	WN	253,791	459.6	8	9	1.154	0.380	0.201	0.238	14,441	0.057	0.241
	WS	51,104	566.6	12	80	1.539	0.493	0.314	0.457	17,780	0.348	0.163
	Total	673,159	2320.6	39	190					83,685	0.124	0.234
1999/00	EN	57,594	241.1	5	9	1.746	0.519	0.349	0.545	5,412	0.094	0.355
	ES	24,811	179.8	7	9	1.818	0.472	0.307	0.509	3,701	0.149	0.215
	WN	111,634	349.9	6	2	1.766	0.458	0.292	0.477	1,954	0.018	0.658
	WS	20,806	243.0	7	7	1.302	0.466	0.276	0.358	1,417	0.068	0.392
	Total	214,845	1013.8	25	27					12,485	0.058	0.207
2000/01	EN	128,773	378.2	11	2	2.094	0.518	0.361	0.618	1,972	0.015	0.546
	ES	29,329	304.0	11	19	2.954	0.544	0.421	0.774	6,398	0.218	0.315
	Total	158,102	682.2	22	21					8,370	0.053	0.275

Table 4b. (D1, 2; A1) Abundance estimates of minke whales obtained from the Passing mode data in Area 2 using the strata boundaries in the standard dataset. Only the definite duplicates were used. The symbols are the same as in the caption of

Area 2	Stratum	Area	L	nL	ns	E(s)	g(0)	esw_s	esw_w	P	D	CV
CP II												
1986/87	EBAY	15,390	125.8	4	40	3.707	0.571	0.380	0.708	24,053	1.563	0.395
	EM	70,405	431.2	3	75	2.963	0.532	0.330	0.602	55,192	0.784	0.277
	EN	125,810	427.7	3	45	2.773	0.476	0.260	0.488	71,312	0.567	0.402
	ES1	23,142	277.4	5	20	3.454	0.490	0.273	0.540	10,527	0.455	0.638
	ES2	45,753	710.0	16	114	3.379	0.550	0.343	0.634	36,227	0.792	0.252
	WBAY	11,591	31.8	1	11	2.037	0.479	0.247	0.410	16,453	1.419	0.601
	WN	95,903	201.0	2	2	2.693	0.517	0.295	0.528	4,360	0.045	1.114
	WS1	10,270	91.7	2	14	1.781	0.400	0.176	0.290	7,944	0.774	0.443
	WS2	21,323	259.6	4	7	2.405	0.444	0.221	0.393	2,982	0.140	0.306
	WS3	79,608	839.0	14	82	2.142	0.461	0.240	0.417	35,107	0.441	0.247
	Total	499,193	3395.1	54	410					264,155	0.529	0.158
CP III												
1996/97	EN	243,784	660.7	17	25	1.410	0.423	0.246	0.350	26,619	0.109	0.334
	ES	52,998	665.6	18	37	1.757	0.534	0.374	0.576	6,928	0.131	0.376
	WN	114,459	194.0	5	8	1.405	0.479	0.293	0.404	11,397	0.100	0.736
	WS	23,233	230.0	8	40	1.572	0.456	0.286	0.436	11,120	0.479	0.211
	Total	434,474	1750.3	48	110					56,064	0.234	0.232
1997/98	ES1	47,407	385.2	8	48	1.721	0.453	0.286	0.460	17,957	0.379	0.475
	ES2	10,545	142.8	5	24	1.898	0.521	0.353	0.572	4,769	0.452	0.757
	WN	52,492	253.3	4	5	1.148	0.388	0.209	0.246	2,857	0.054	0.321
	WS	32,863	303.2	10	1	1.631	0.529	0.365	0.541	243	0.007	0.923
	EN1	85,391	345.1	6	9	1.380	0.482	0.298	0.403	5,191	0.061	0.282
	EN2	80,645	258.6	4	7	1.299	0.436	0.257	0.337	5,618	0.070	0.393
	Total	309,343	1688.3	37	94					36,635	0.118	0.269
1999/00	ENA	7,443	34.2	2	0	-		-		0	0	0
	ESA	6,540	54.6	2	0	-		-		0	0	0
	Total	13,983	88.8	4	0					0	0	0

Table 4c. (D1, 2; A1) Abundance estimates of minke whales obtained from the Passing mode data in Area 3 using the strata boundaries in the standard dataset. Only the definite duplicates were used. The symbols are the same as in the caption of Table

Area 3	Stratum	Area	L	nL	ns	E(s)	g(0)	esw_s	esw_w	P	D	CV
CP II												
1987/88	EN	170,714	514.5	7	8	2.154	0.486	0.256	0.443	11,253	0.066	0.484
	ES	88,908	666.3	8	48	1.956	0.511	0.281	0.455	22,511	0.253	0.492
	WN	149,642	358.0	7	35	3.057	0.547	0.329	0.594	68,118	0.455	0.447
	WS	75,367	486.9	9	121	2.648	0.507	0.281	0.510	88,470	1.174	0.216
	Total	484,631	2025.8	31	212					190,352	0.393	0.207
CP III												
1992/93	EN	151,683	562.2	5	10	1.549	0.437	0.263	0.401	8,032	0.053	0.533
	ES	23,240	487.5	13	18	1.934	0.552	0.404	0.639	2,043	0.088	0.366
	WN	209,976	775.1	7	42	1.934	0.552	0.403	0.644	27,367	0.130	0.377
	WS	61,799	893.7	15	157	1.794	0.477	0.314	0.513	31,202	0.505	0.219
	Total	446,698	2718.4	40	227					68,644	0.154	0.195
1994/95	WN	149,903	457.9	7	21	1.352	0.412	0.236	0.325	19,977	0.133	0.331
	WS	52,353	505.3	11	52	1.971	0.536	0.377	0.609	14,037	0.268	0.449
	ESW	69,854	318.0	4	17	1.338	0.462	0.271	0.361	9,265	0.133	0.514
	ENW	34,123	234.2	4	32	1.546	0.428	0.252	0.385	14,387	0.422	0.517
	Total	306,233	1515.4	26	122					44,540	0.145	0.227

Table 4d. (D1, 2; A1) Abundance estimates of minke whales obtained from the Passing mode data in Area 4 using the strata boundaries in the standard dataset. Only the definite duplicates were used. The symbols are the same as in the caption of Table

Area 4	Stratum	Area	L	nL	ns	E(s)	g(0)	esw_s	esw_w	P	D	CV
CP II												
1988/89	BN	17,812	412.9	10	28	2.360	0.486	0.254	0.451	5,623	0.316	0.255
	BS	6,637	144.5	3	50	2.793	0.557	0.348	0.613	9,271	1.397	0.744
	EN	181,449	606.0	6	17	1.940	0.490	0.252	0.411	19,658	0.108	0.262
	ES	54,149	255.8	7	49	1.907	0.470	0.238	0.393	41,885	0.774	0.233
	WN	156,058	716.6	6	5	2.114	0.477	0.244	0.420	4,737	0.030	0.450
	WS	60,925	245.7	5	23	2.252	0.507	0.273	0.468	23,482	0.385	0.348
	Total	477,030	2381.6	37	172					104,657	0.219	0.160
CP III												
1994/95	PRYD	77,912	312.7	4	5	1.375	0.484	0.300	0.405	2,877	0.037	0.420
	ESE	25,768	225.3	4	17	1.340	0.390	0.208	0.288	6,250	0.243	0.608
	ENE	21,909	203.5	4	48	1.312	0.392	0.211	0.286	16,118	0.736	0.326
	Total	125,589	741.4	12	70					25,246	0.201	0.268
1998/99	EN	170,569	578.7	14	21	1.112	0.456	0.265	0.296	13,007	0.076	0.226
	ES	70,855	685.9	25	34	1.227	0.407	0.228	0.286	9,510	0.134	0.183
	WN	106,192	377.9	10	29	1.845	0.483	0.323	0.534	23,269	0.219	1.022
	WS	43,071	472.4	15	32	2.552	0.582	0.457	0.776	8,080	0.188	0.340
	Total	390,687	2114.8	64	116					53,866	0.138	0.451

Table 4e. (D1, 2; A1) Abundance estimates of minke whales obtained from the Passing mode data in Area 5 using the strata boundaries in the standard dataset. Only the definite duplicates were used. The symbols are the same as in the caption of Table

Area 5	Stratum	Area	L	nL	ns	E(s)	g(0)	esw_s	esw_w	P	D	CV
CP II												
1985/86	EM	166,143	1041.2	10	182	2.594	0.521	0.302	0.534	125,369	0.755	0.346
	EN	279,619	844.0	8	68	2.443	0.460	0.240	0.442	115,567	0.413	0.340
	ES	107,553	739.2	8	191	2.586	0.492	0.271	0.493	133,212	1.239	0.278
	WM	166,349	492.0	4	53	2.007	0.481	0.249	0.414	72,350	0.435	0.533
	WN	139,080	357.6	3	59	1.889	0.464	0.239	0.392	91,557	0.658	0.440
	WS	104,814	647.6	13	103	2.367	0.452	0.232	0.424	85,716	0.818	0.180
	Total	963,558	4121.6	46	656					623,771	0.647	0.157
CP III												
1991/92	EN	165,429	505.8	8	118	1.991	0.554	0.405	0.657	95,037	0.574	0.181
	ES	82,237	687.5	10	106	1.905	0.478	0.315	0.533	38,546	0.469	0.384
	WN	137,992	337.1	5	9	2.417	0.524	0.384	0.686	11,598	0.084	0.731
	WS	58,358	470.8	5	174	2.315	0.569	0.431	0.729	58,085	0.995	0.515
	Total	444,016	2001.3	28	407					203,266	0.458	0.194
2001/02	EN	83,701	295.0	4	4	1.844	0.477	0.314	0.521	3,346	0.040	0.379
	ES	26,316	231.9	8	39	1.445	0.489	0.312	0.435	10,332	0.393	0.286
	WN	46,668	184.1	3	4	1.039	0.373	0.195	0.204	2,701	0.058	0.775
	WS	35,155	301.6	11	25	2.057	0.553	0.410	0.649	7,166	0.204	0.502
	Total	191,840	1012.7	26	72					23,545	0.123	0.229
2002/03	EN	136,035	541.3	16	16	1.256	0.428	0.249	0.318	10,203	0.075	0.193
	ES	127,980	536.0	12	39	1.486	0.512	0.339	0.476	20,336	0.159	0.444
	W1N	75,957	244.6	7	25	1.292	0.420	0.243	0.319	20,698	0.272	0.198
	W1S	22,305	228.5	7	27	3.010	0.598	0.489	0.851	7,646	0.343	0.306
	W2N	101,810	284.4	9	13	1.590	0.489	0.320	0.479	11,786	0.116	0.518
	W2S	21,741	257.1	14	20	1.453	0.438	0.265	0.383	4,666	0.215	0.183
	Total	485,828	2091.9	65	140					75,335	0.155	0.169
2003/04	MID	133,059	909.9	21	235	2.184	0.534	0.391	0.661	96,949	0.729	0.205
	N1	124,129	167.7	7	4	3.095	0.553	0.433	0.798	10,622	0.086	0.409
	N2	96,296	274.8	9	25	2.273	0.574	0.442	0.733	22,459	0.233	0.547
	N3	15,314	126.4	4	42	1.993	0.557	0.411	0.658	12,254	0.800	0.205
	ROSS	57,045	575.8	19	139	1.900	0.516	0.362	0.588	36,399	0.638	0.139
	Total	421,496	2054.6	60	445					163,791	0.389	0.143

Table 4f. (D1, 2; A1) Abundance estimates of minke whales obtained from the Passing mode data in Area 6 using the strata boundaries in the standard dataset. Only the definite duplicates were used. The symbols are the same as in the caption of Table

Area 6	Stratum	Area	L	nL	ns	E(s)	g(0)	esw_s	esw_w	P	D	CV
CP II												
1990/91	EN	193,259	473.6	4	24	1.567	0.457	0.214	0.313	35,887	0.186	0.582
	ES	109,335	476.3	4	27	1.894	0.455	0.220	0.362	26,687	0.244	0.325
	WN	213,366	551.4	4	19	1.852	0.453	0.216	0.353	31,571	0.148	0.385
	WS	45,803	645.9	9	42	2.613	0.527	0.300	0.528	12,933	0.282	0.246
	Total	561,763	2147.2	21	112					107,078	0.191	0.250
CP III												
1995/96	EN	243,930	533.5	11	32	1.544	0.499	0.320	0.468	35,467	0.145	0.248
	ES	72,931	561.8	10	46	1.291	0.404	0.226	0.299	17,224	0.236	0.292
	WN	98,623	280.3	5	13	1.301	0.384	0.202	0.273	14,700	0.149	0.331
	WS	34,475	314.1	9	5	1.414	0.473	0.285	0.397	1,368	0.040	0.296
	Total	449,959	1689.7	35	96					68,759	0.153	0.172
2000/01	WN	254,027	459.2	13	18	1.602	0.488	0.320	0.482	25,122	0.099	0.334
	WS	44,283	417.6	17	48	1.529	0.494	0.324	0.470	12,129	0.274	0.205
	Total	298,310	876.8	30	66					37,251	0.125	0.238

Table 5. (A2) Abundance estimates of minke whales obtained from the Passing mode data using the additional variance blocks with the common northern boundary for additional variance estimation. Only the definite duplicates were used.

		CPII						CPIII											
Area	Sector	1986	1987	1988	1989	1990	1991	1993	1994	1995	1996	1997	1998	1999	2000	2001	2002	2003	2004
1	W					61,346										7,020			
						0.333										0.401			
	M					107,301			26,169										
						0.439			0.188										
	E					27,541			38,392						7,138				
						0.418			0.387						0.233				
2	W		46,031										37,475						
			0.282										0.296						
	E		120,021									42,610							
			0.257									0.264							
3	W			138,349				43,633											
				0.240				0.161											
	E			26,505						49,951									
				0.520						0.281									
4	W				27,456					24,024									
					0.399					0.294									
	E				59,069									49,677					
					0.257									0.437					
5	W	115,297															24,594		
		0.236															0.226		
	M	120,006																46,943	
		0.349																0.166	
	E	296,262																	172,246
		0.227																	0.149
6	W						43,172				68,226								
							0.292				0.177								
	E						45,561									31,461			
							0.425									0.212			

Table 6. (A3) Abundance estimates of minke whales obtained from the Passing mode data using the additional variance blocks without the common northern boundary. Only the definite duplicates were used.

		CPII						CPIII											
Area	Sector	1986	1987	1988	1989	1990	1991	1993	1994	1995	1996	1997	1998	1999	2000	2001	2002	2003	2004
1	W					61,346										8,300			
						0.323										0.275			
	M					115,220			44,752										
						0.314			0.214										
	E					32,623			40,847						11,996				
						0.321			0.468						0.212				
2	W		52,873										36,345						
			0.274										0.269						
	E		208,183									57,004							
			0.180									0.304							
3	W			160,816				68,584											
				0.231				0.195											
	E			26,024						57,227									
				0.465						0.227									
4	W				27,111					25,041									
					0.382					0.268									
	E				77,040									53,469					
					0.182									0.451					
5	W	140,449															23,363		
		0.202															0.229		
	M	165,897																48,928	
		0.295																0.166	
	E	328,414																	171,693
		0.183																	0.145
6	W						44,168				68,221								
							0.285				0.172								
	E						45,560									36,955			
							0.425									0.238			

Table 7. Variance-covariance matrix for abundance estimates of minke whales obtained from the IO mode data using the additional variance blocks for additional variance estimation. Only the definite duplicates were used.

	1986.5M	1986.5W	1987.2E	1987.2W	1988.3E	1988.3W	1989.4E	1989.4W	1990.1E	1990.1M	1990.1W	1991.6E	1991.6W
1986.5E	0.079	0.099	0.086	0.062	0.011	0.065	0.076	0.041	0.065	0.027	0.037	0.036	0.048
1986.5M		0.168	0.127	0.088	0.024	0.113	0.139	0.062	0.140	0.036	0.078	0.063	0.096
1986.5W			0.169	0.135	0.028	0.122	0.163	0.065	0.183	0.033	0.088	0.071	0.106
1987.2E				0.101	0.020	0.104	0.123	0.059	0.116	0.040	0.069	0.055	0.079
1987.2W					0.013	0.062	0.079	0.036	0.082	0.019	0.039	0.038	0.053
1988.3E						0.020	0.025	0.010	0.027	0.005	0.015	0.011	0.017
1988.3W							0.118	0.059	0.107	0.039	0.067	0.055	0.081
1989.4E								0.068	0.158	0.037	0.078	0.069	0.100
1989.4W									0.056	0.024	0.032	0.034	0.045
1990.1E										0.021	0.080	0.067	0.101
1990.1M											0.170	0.018	0.024
1990.1W												0.031	0.054
1991.6E													0.048

	1994.1E	1994.1M	1995.3E	1995.4W	1996.6W	1997.2E	1998.2W	1999.4E	2000.1E	2001.1W	2001.6E	2002.5W	2003.5M	2003.5E
1993.3W	0.015	0.118	0.073	0.067	0.101	0.056	0.061	0.037	0.074	0.042	0.066	0.070	0.097	0.093
1994.1E		0.025	0.017	0.014	0.025	0.012	0.012	0.007	0.018	0.007	0.012	0.015	0.014	0.019
1994.1M			0.148	0.158	0.202	0.105	0.115	0.055	0.135	0.071	0.092	0.102	0.149	0.129
1995.3E				0.096	0.128	0.066	0.071	0.034	0.086	0.042	0.058	0.066	0.090	0.082
1995.4W					0.131	0.066	0.073	0.031	0.084	0.043	0.050	0.056	0.087	0.068
1996.6W						0.092	0.098	0.047	0.121	0.055	0.080	0.094	0.121	0.114
1997.2E							0.052	0.027	0.062	0.030	0.047	0.052	0.071	0.064
1998.2W								0.029	0.066	0.035	0.050	0.054	0.079	0.068
1999.4E									0.034	0.019	0.033	0.035	0.049	0.044
2000.1E										0.041	0.059	0.068	0.086	0.087
2001.1W											0.033	0.033	0.052	0.050
2001.6E												0.064	0.090	0.080
2002.5W													0.091	0.087
2003.5M														0.112

Table 8. (A4, 5) Abundance estimates for each Management Area and the circumpolar estimates for CP II and III with the additional CV. Only the definite duplicates were used.

additional CV 0.413

survey once	Area	I	II	III	IV	V	VI	Total
CP II	Area size	429,736	493,258	480,841	473,477	960,973	502,901	3,341,187
	Abundance	**209,188**	**261,056**	**186,841**	**104,151**	**634,760**	**89,728**	**1,485,724**
	Density	0.487	0.529	0.389	0.220	0.661	0.178	0.445
	CV	0.219	0.159	0.211	0.173	0.142	0.263	0.098
	CV with add.var	0.345	0.375	0.418	0.367	0.293	0.393	0.172
CP III	Area size	817,066	727,790	749,500	512,438	828,924	742,449	4,378,167
	Abundance	**65,047**	**93,349**	**125,810**	**78,510**	**243,985**	**105,176**	**711,877**
	Density	0.080	0.128	0.168	0.153	0.294	0.142	0.163
	CV	0.164	0.218	0.154	0.322	0.115	0.145	0.089
	CV with add.var	0.341	0.370	0.331	0.447	0.326	0.338	0.165
Ratio of abund.		0.31	0.36	0.67	0.75	0.38	1.17	0.48
Ratio of dens.		0.16	0.24	0.43	0.70	0.45	0.79	0.37

Table 9. Comparison of abundances between with-Platform C and without-Platform C.

Year	Area	with Platform C	without Platform C	Ratio without_C/with_C
1986	5	623,771	521,454	0.84
1987	2	264,155	241,373	0.91
1988	3	190,352	151,742	0.80
1989	4	104,657	70,968	0.68
1990	1	198,048	173,232	0.87
1991	6	107,078	67,055	0.63
1992	5	203,266	183,305	0.90
1993	3	68,644	62,484	0.91
1994	1	83,685	62,547	0.75
1995	3	57,666	51,163	0.89
1995	4	25,246	20,199	0.80
1996	6	68,759	53,119	0.77
1997	2	56,064	50,837	0.91
1998	2	36,635	32,999	0.90
1999	4	53,866	52,549	0.98
2000	1	12,485	9,817	0.79
2000	2	0	0	-
2001	1	8,370	8,865	1.06
2001	6	37,251	29,460	0.79
2002	5	23,545	22,630	0.96
2003	5	75,335	57,654	0.77
2004	5	178,683	176,506	0.99

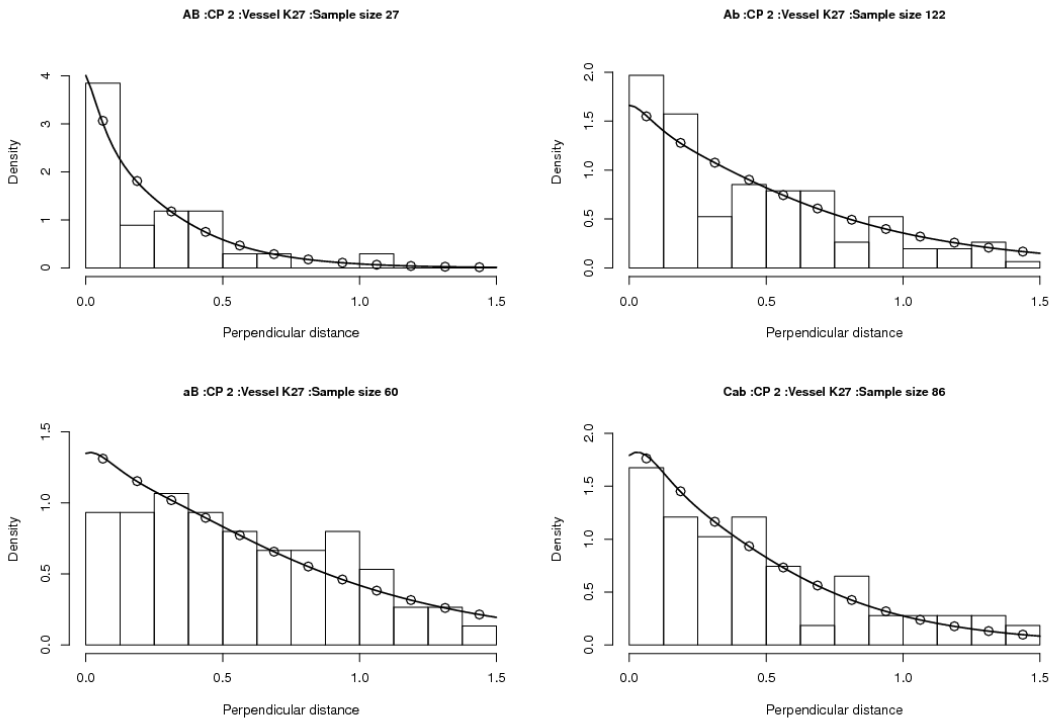

Fig. 1a. Plots for perpendicular distance of IO mode and vessel K27 in CP2.

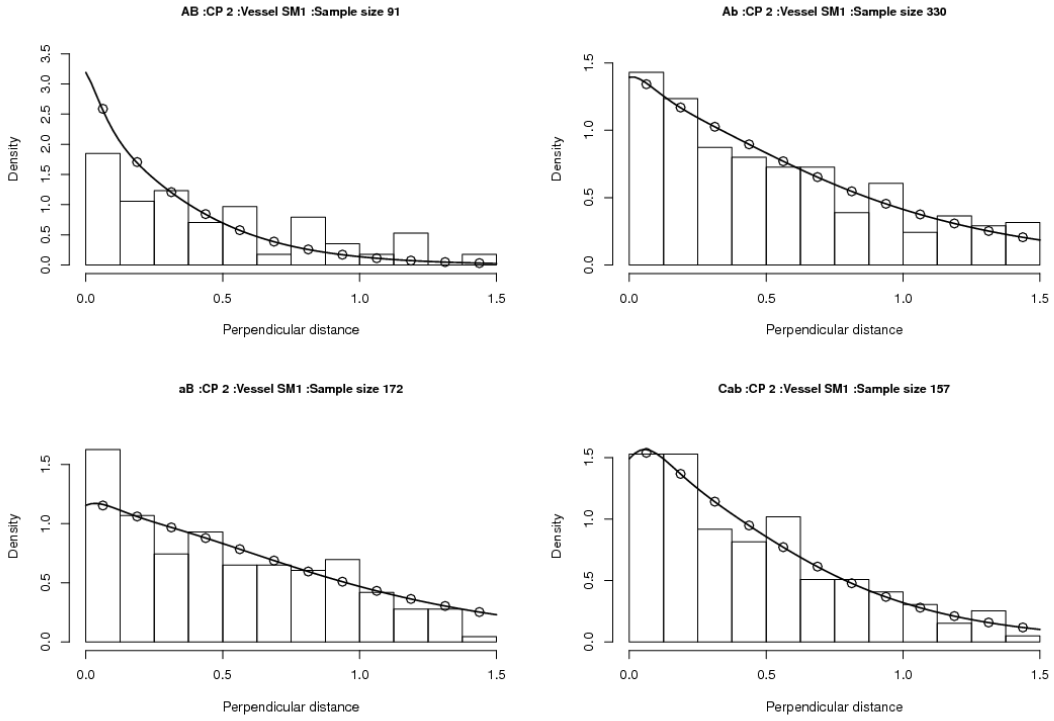

Fig. 1b. Plots for perpendicular distance of IO mode and vessel SM1 in CP2.

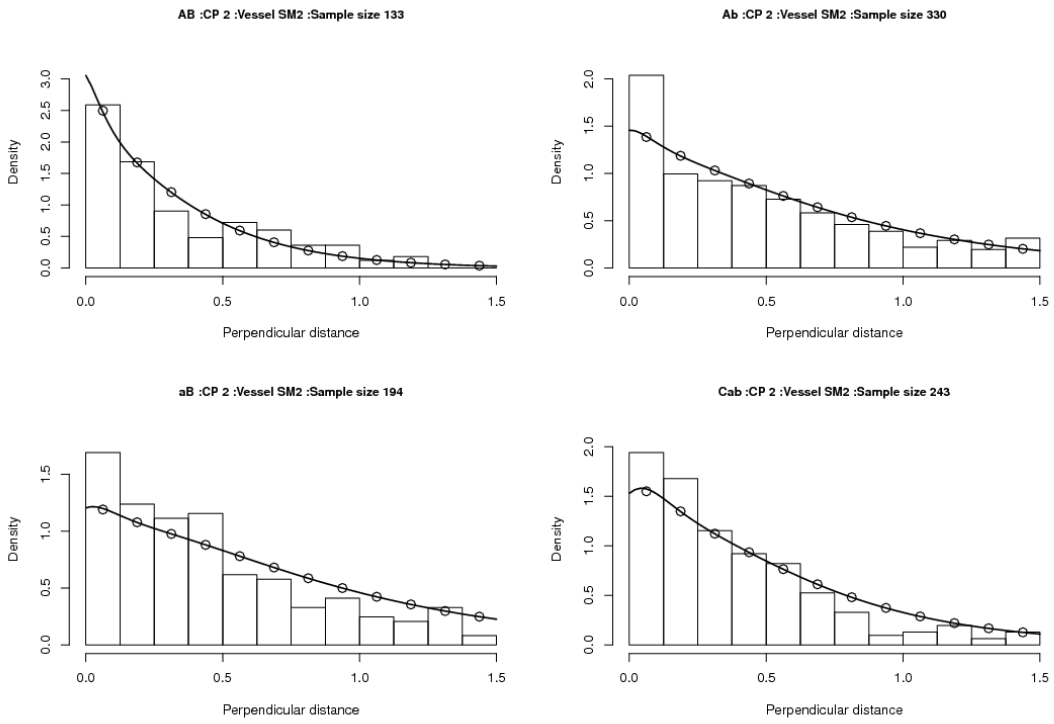

Fig. 1c. Plots for perpendicular distance of IO mode and vessel SM2 in CP2.

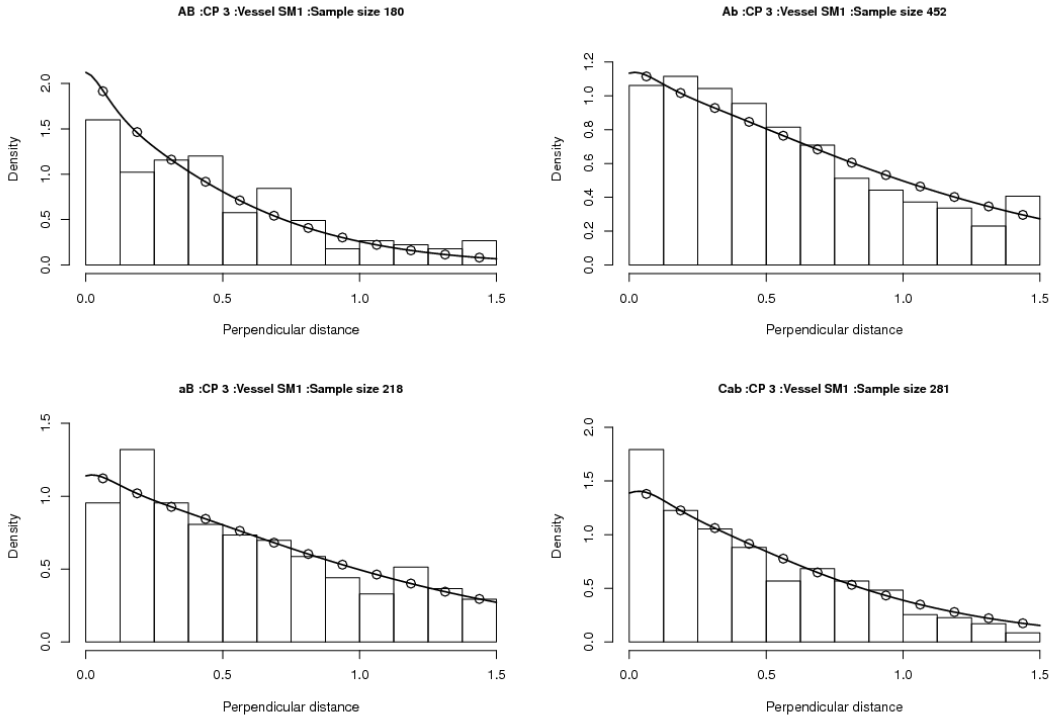

Fig. 1d. Plots for perpendicular distance of IO mode and vessel SM1 in CP3.

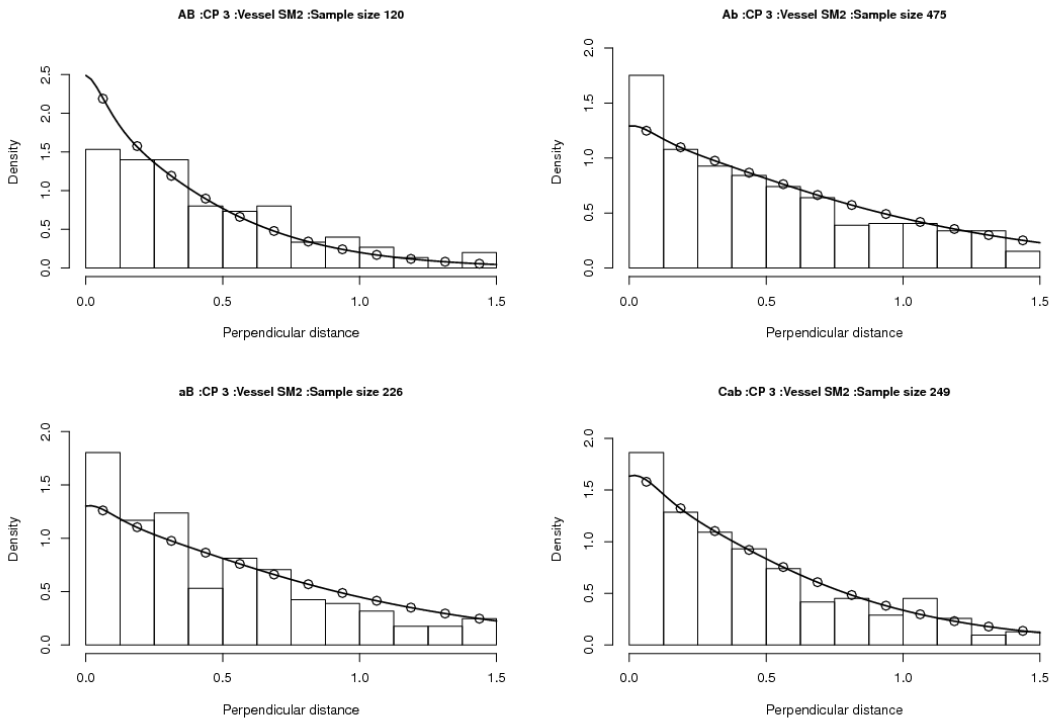

Fig. 1e. Plots for perpendicular distance of IO mode and vessel SM2 in CP3.

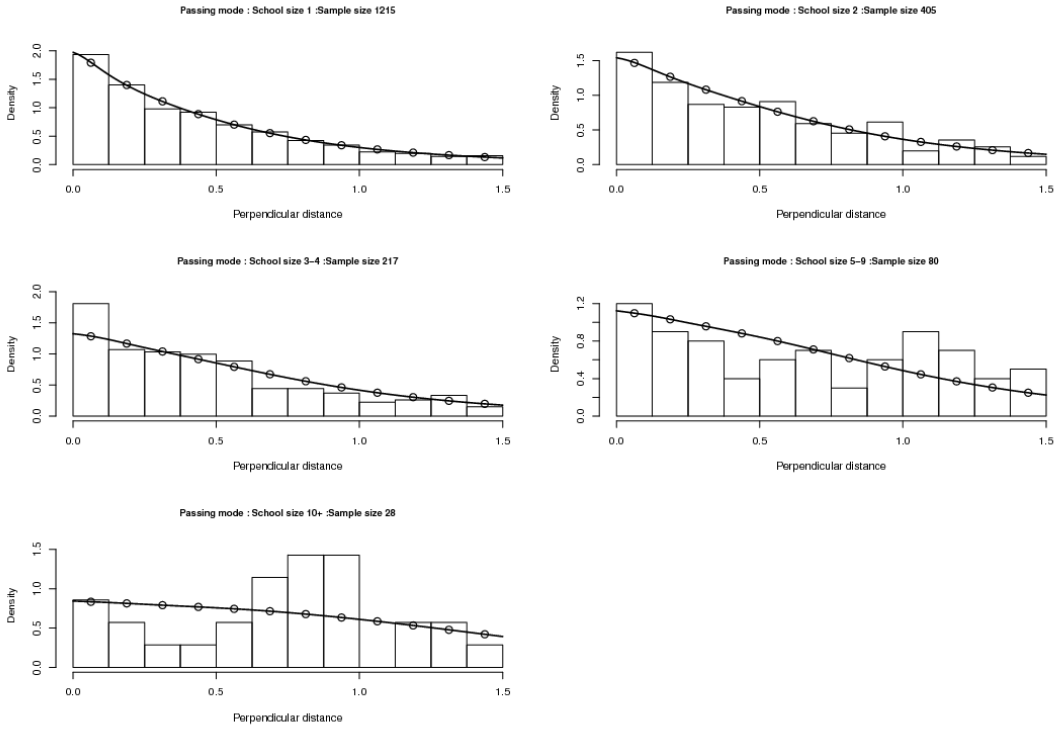

Fig. 2a. Plots for perpendicular distance of IO Passing mode by school size in CP2.

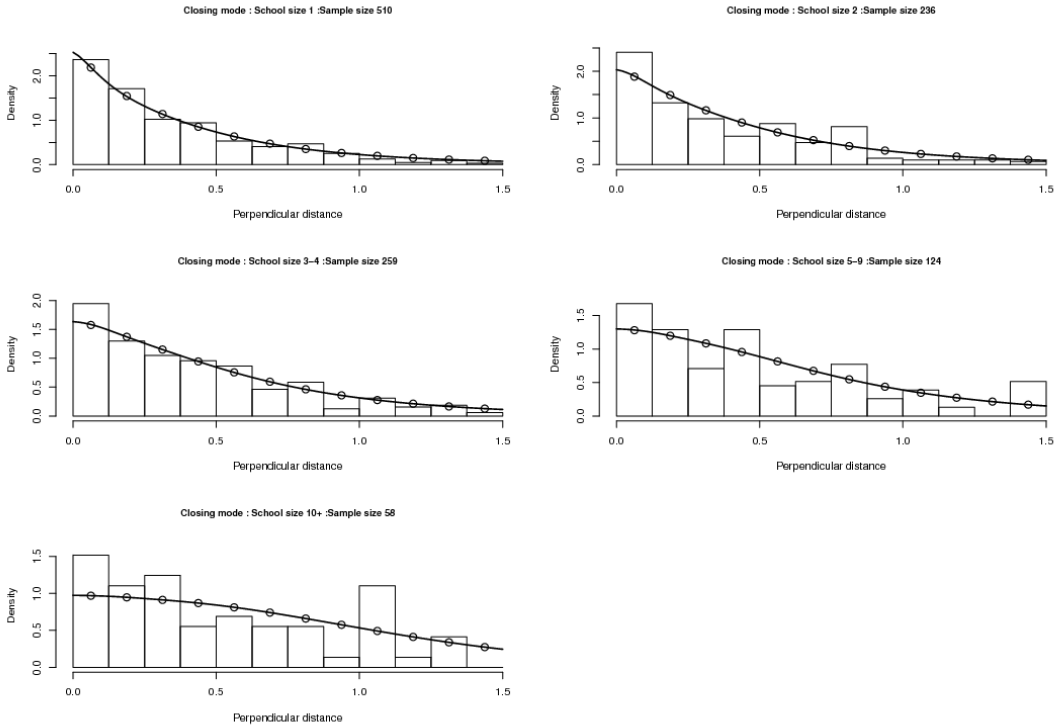

Fig. 2b. Plots for perpendicular distance of Closing mode by school size in CP2.

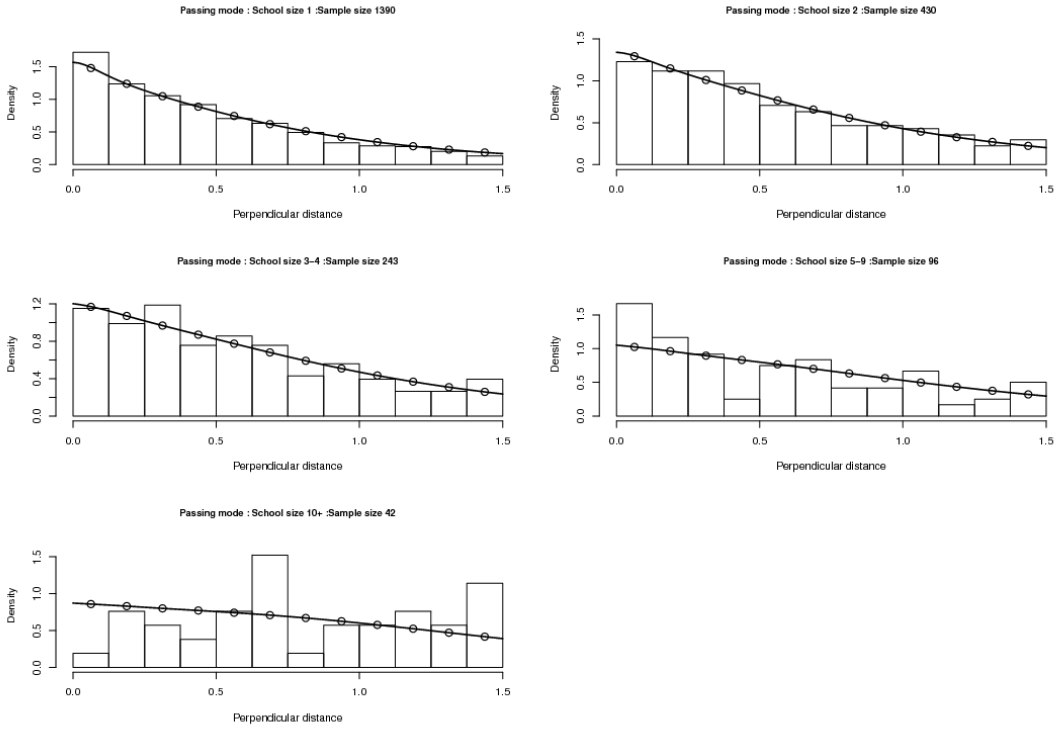

Fig. 2c. Plots for perpendicular distance of IO Passing mode by school size in CP3.

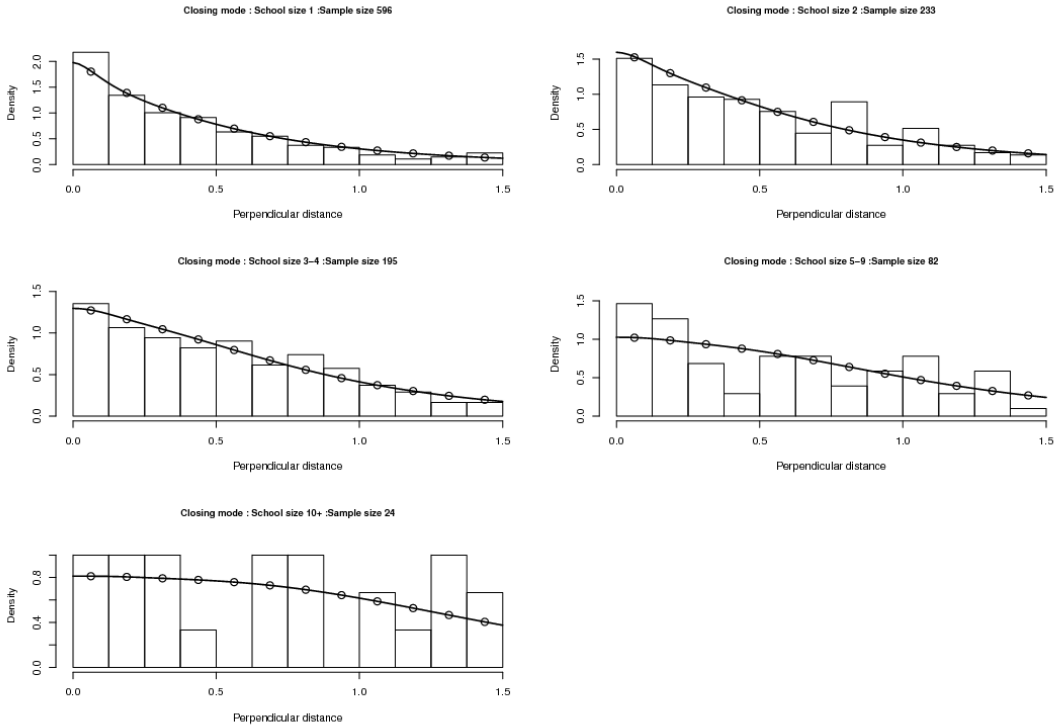

Fig. 2d. Plots for perpendicular distance of Closing mode by school size in CP3.

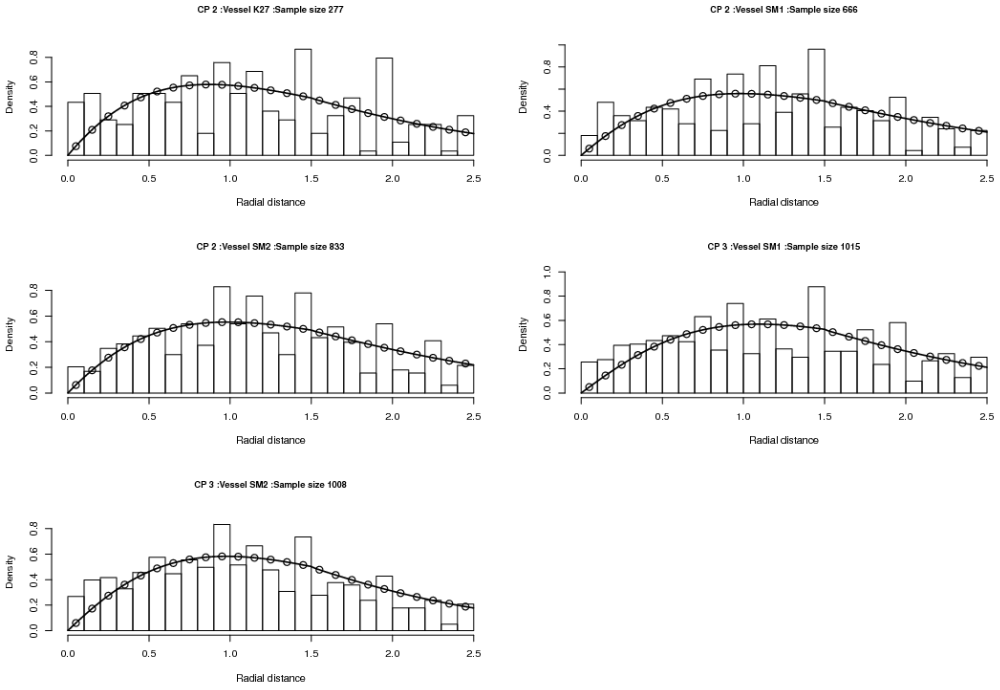

Fig. 3. Plots for radial distance of IO Passing mode by vessel. The first three are CP2 and the latter two are CP3.

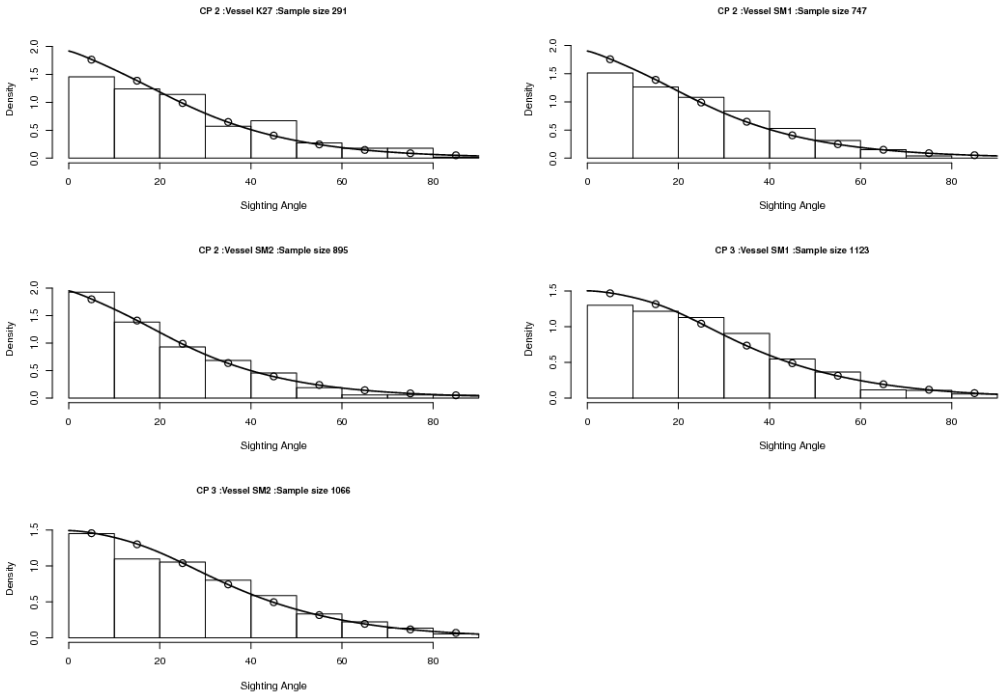

Fig. 4. Plots for sighting angle of IO Passing mode by vessel. The first three are CP2 and the latter two are CP3.

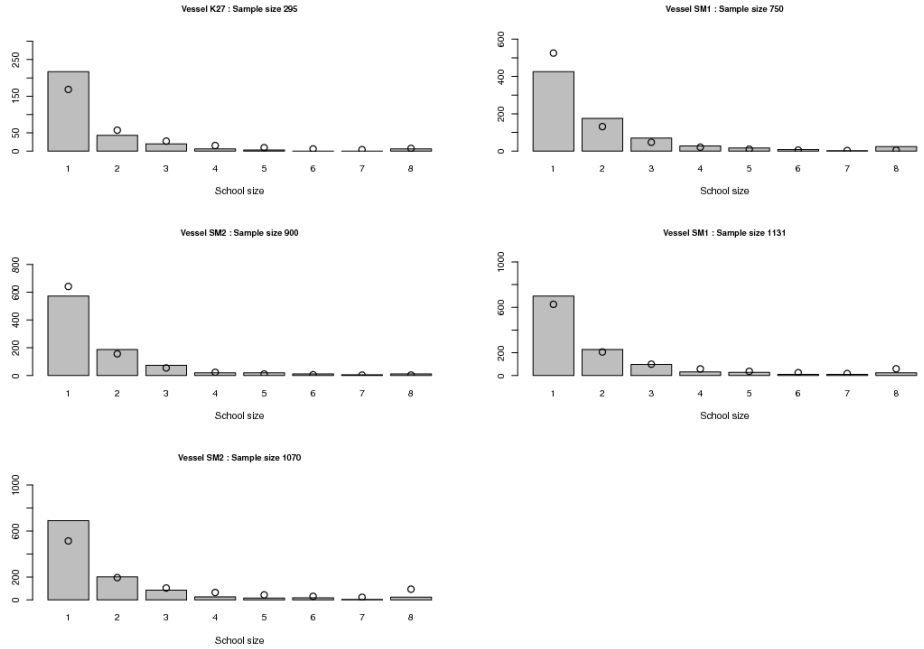

Fig 5a. Plots for school size of IO Passing mode by vessel. The first three are CP2 and the latter two are CP3.

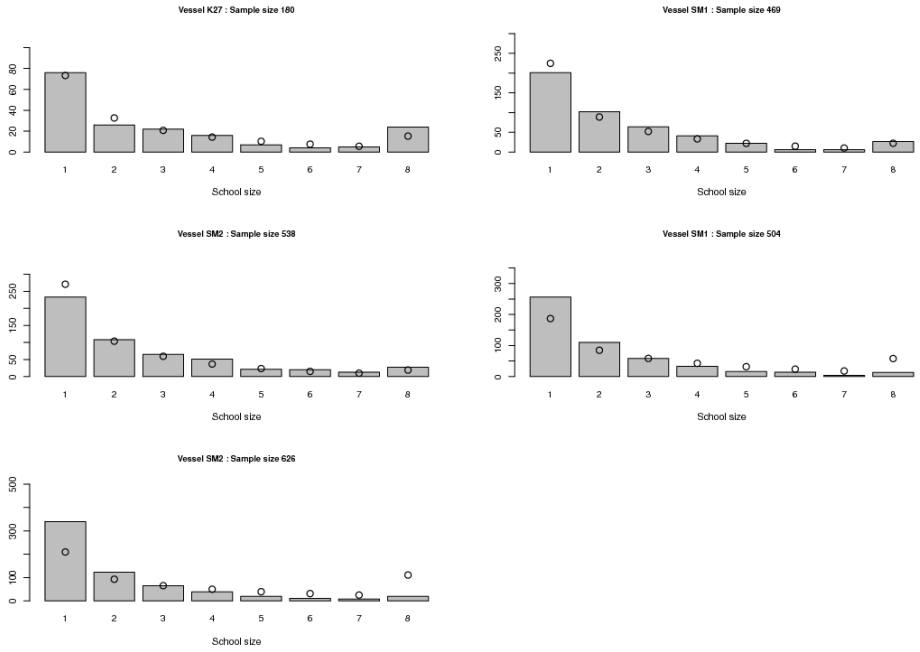

Fig 5b. Plots for school size of Closing mode by vessel. The first three are CP2 and the latter two are CP3.

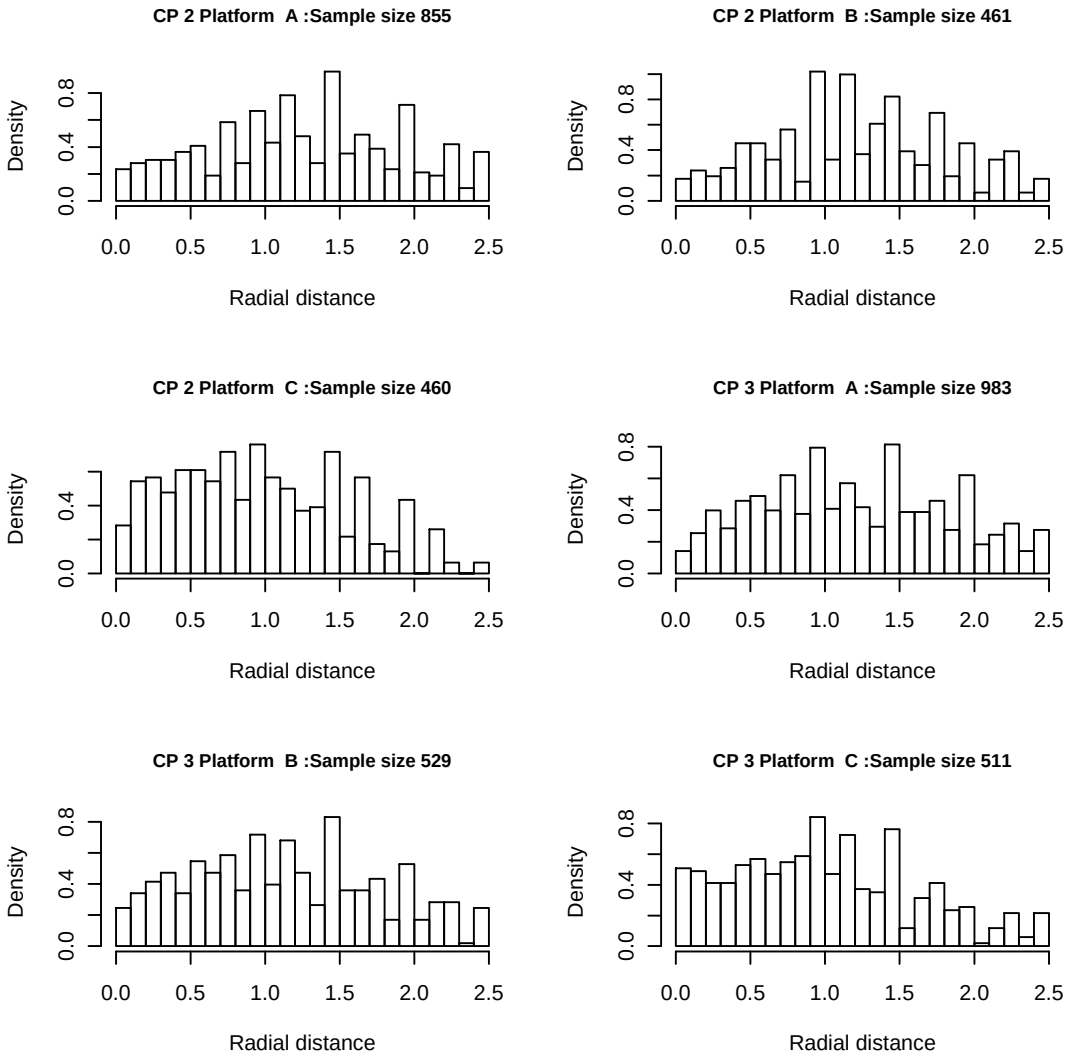

Fig.6a. Plots of radial distance by platform for IO mode data.

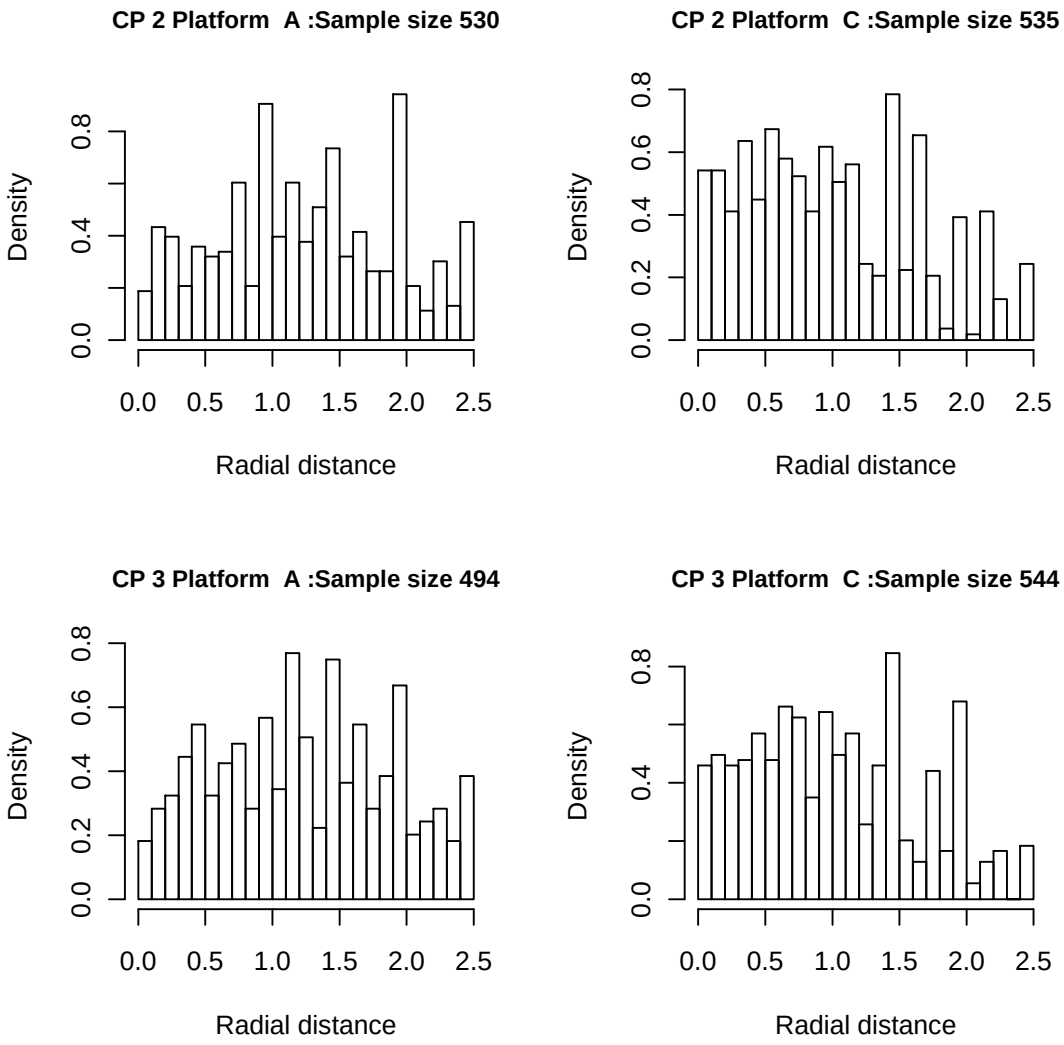

Fig. 6b. Plots of radial distance by platform for CL mode data.

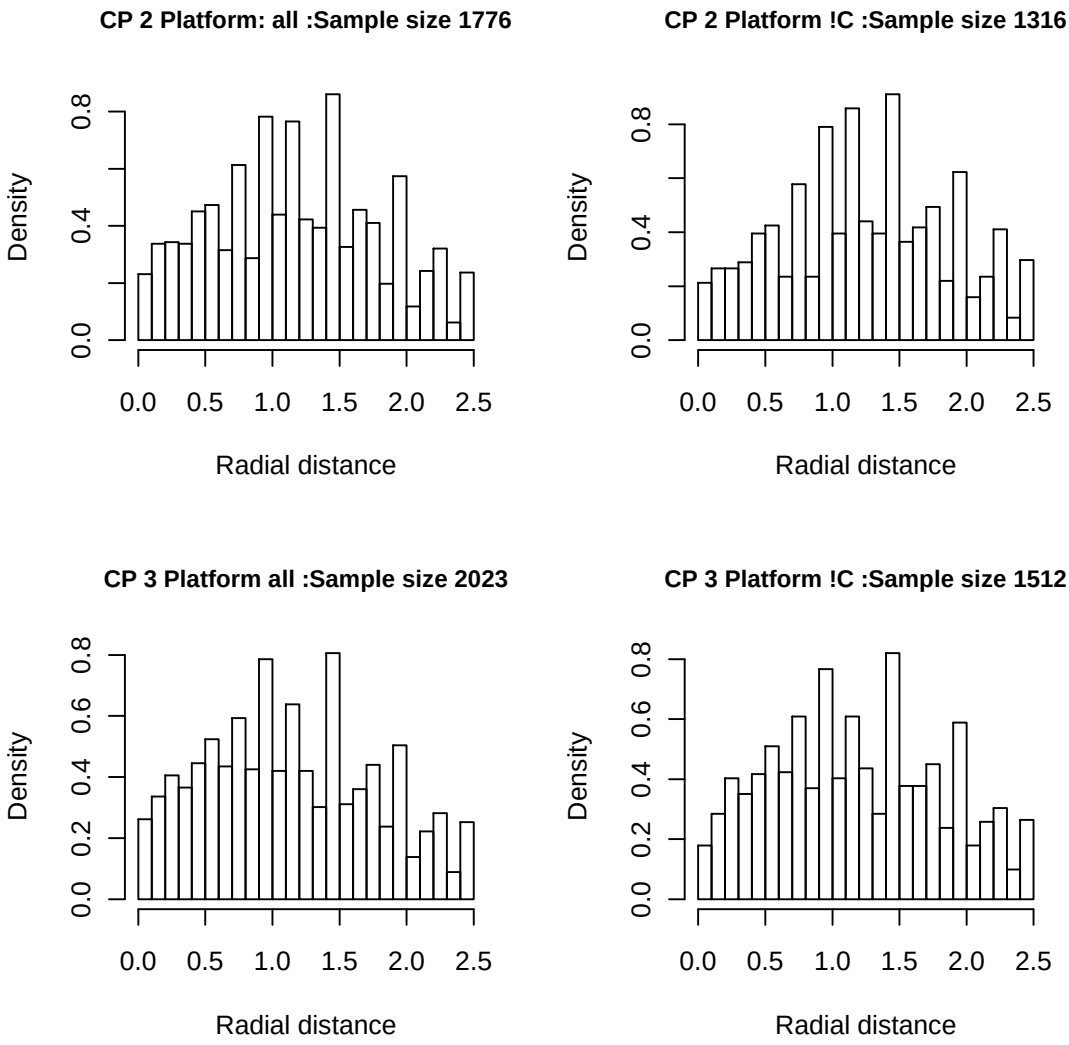

Fig. 7a. Plots of radial distance with and without Platform C for IO mode data.

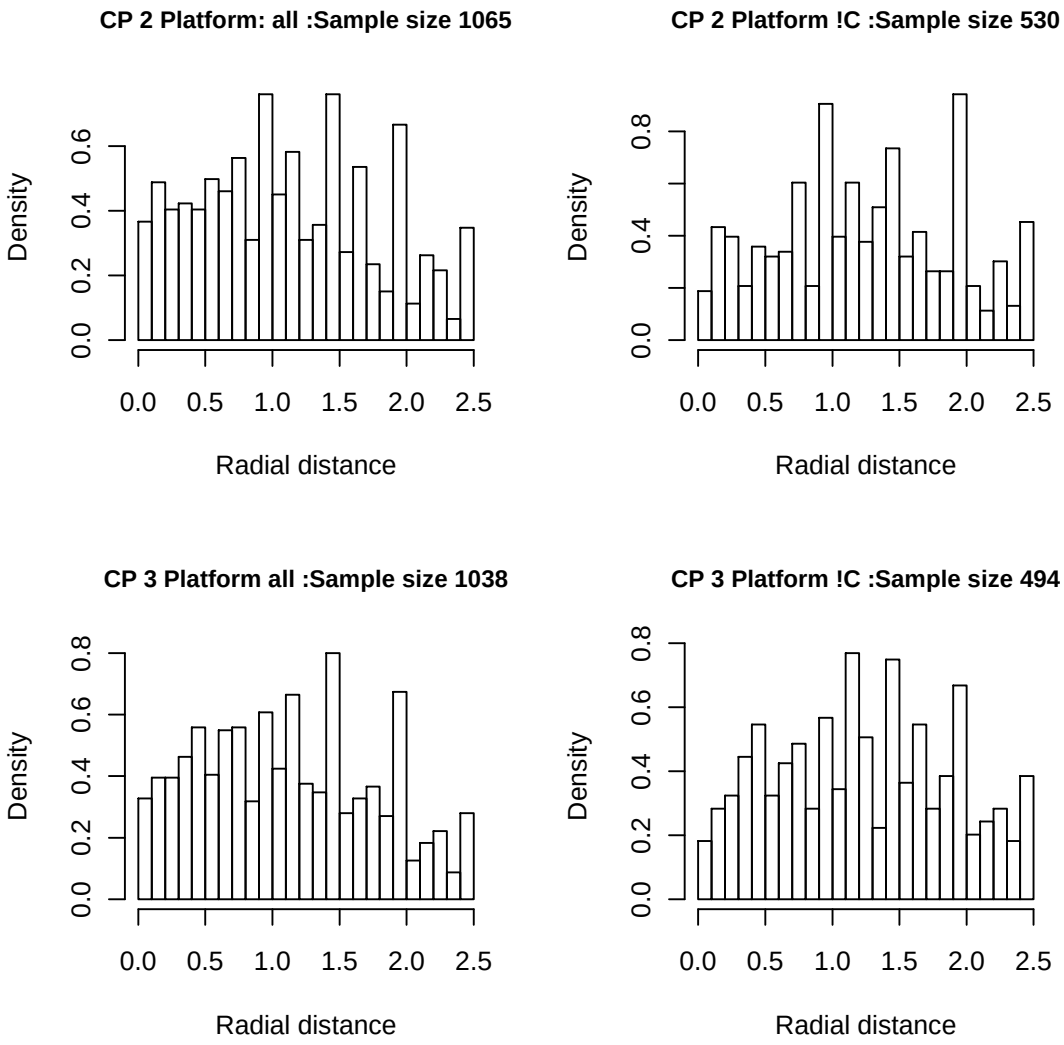

Fig. 7b. Plots of radial distance with and without Platform C for CL mode data.

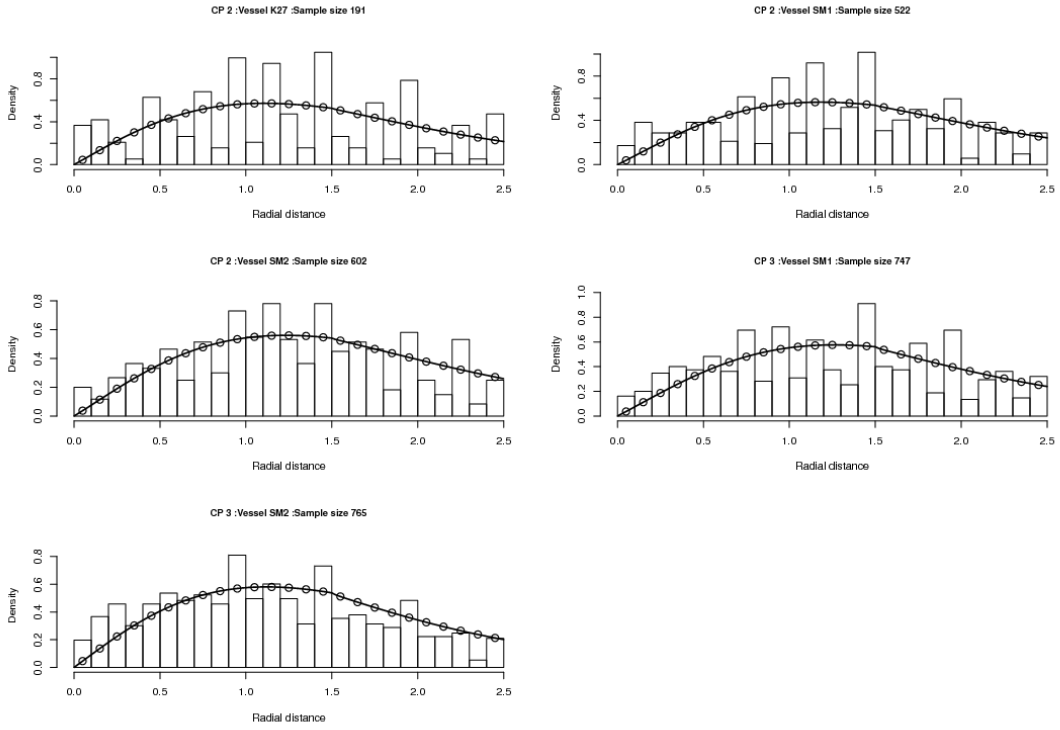

Fig. 8. Plots of radial distance by vessel when Platform C was eliminated. The circles and solid lines are prediction by the model. The first three are CP2 and